

Reaction of cyanoacetylene $\text{HCCCN}(X^1\Sigma^+)$ with ground-state carbon atoms $\text{C}(^3P)$ in cold molecular clouds

H. Y. Li, W. C. Cheng, Y. L. Liu, B. J. Sun, C. Y. Huang, K. T. Chen, and M. S. Tang
Department of Chemistry, National Dong Hwa University, Shoufeng, Hualien 974, Taiwan, Republic of China

R. I. Kaiser
Department of Chemistry, University of Hawaii at Manoa, Honolulu, Hawaii 96822

A. H. H. Chang^{a)}
Department of Chemistry, National Dong Hwa University, Shoufeng, Hualien 974, Taiwan, Republic of China

(Received 24 August 2005; accepted 10 November 2005; published online 25 January 2006)

The reaction of the simplest cyanopolyne, cyanoacetylene [$\text{HCCCN}(X^1\Sigma^+)$], with ground-state atomic carbon $\text{C}(^3P)$ is investigated theoretically to explore the probable routes for the depletion of the famed interstellar molecule HCCCN, and the formation of carbon-nitrogen-bearing species in extraterrestrial environments particularly of ultralow temperature. Six collision complexes (c1–c6) without entrance barrier as a result of the carbon atom addition to the π systems of HCCCN are located. The optimized geometries and harmonic frequencies of the intermediates, transition states, and products along the isomerization and dissociation pathways of each collision complex are obtained by utilizing the unrestricted B3YLP/6-311G(*d,p*) level of theory, and the corresponding CCSD(T)/cc-pVTZ energies are calculated. Subsequently, with the facilitation of Rice-Ramsperger-Kassel-Marcus (RRKM) and variational RRKM rate constants at collision energy of 0–10 kcal/mol, the most probable paths for the titled reaction are determined, and the product yields are estimated. Five collision complexes (c1–c3, c5, and c6) are predicted to give the same products, a chained CCCCN (p2)+H, via the linear and most stable intermediate, HCCCCN (i2), while collision complex c4 is likely to dissociate back to C+HCCCN. The study suggests that this class of reaction is an important route to the destruction of cyanoacetylene and cyanopolynes in general, and to the synthesis of linear carbon-chained nitriles at the temperature as low as 10 K to be incorporated in future chemical models of interstellar clouds. © 2006 American Institute of Physics. [DOI: 10.1063/1.2148411]

I. INTRODUCTION

The absolute rate constants for the reactions of the ground-state carbon atom $\text{C}(^3P)$ with unsaturated hydrocarbons, and the cyano radical (CN) with various hydrocarbons at both room^{1–9} and ultralow^{10–12} temperatures were surprisingly found to be of gas-kinetics magnitude. It indicates that the reactions are almost barrierless and would be able to compete with the ion-molecule reactions at ultralow temperature as present in cold molecular clouds (10 K). Owing to the experimental findings, certain types of neutral-neutral reactions are believed to be important in the astronomical environments such as interstellar clouds, where the density is very low and the temperature is at 10–50 K. It follows that fast neutral-neutral reactions have been integrated^{13–16} into chemical models which explain and predict the abundances of species in the interstellar clouds. However, the fact that the kinetic investigations are often based on the consumption of the reactants, so that many neutral-neutral reactions in the model are essentially speculative, hinders the development

of an accurate model. It would therefore be highly desirable to have studies that elucidate reaction paths and products.

The reactions of carbon atom play a particularly important role in the synthesis and growth of complex hydrocarbon molecules. For the reactions of the ground-state carbon atom $\text{C}(^3P)$ with various unsaturated hydrocarbons, studies^{17–30} using crossed-beam experiments or using combined *ab initio* calculations and crossed-beam experiments scrutinized reaction paths and made observation of products. The results reassert the reaction of ubiquitous interstellar carbon atom $\text{C}(^3P)$ with unsaturated hydrocarbon in the reaction networks.

Among the detected interstellar molecules and species in the atmospheres of planets and moons, the nitrogen-bearing nitriles are of potential relevance to the formation of biological molecules.³¹ Intensive investigations^{32–41} have focused on the formation of nitriles through the reactions of CN radical with unsaturated hydrocarbons. On the other hand, as indicated by previous works, the electrophilic $\text{C}(^3P)$ atom would attack the electron-rich π systems of unsaturated hydrocarbons to initiate the reactions. Thus, presumably

^{a)}Fax: +886-3-8633570. Electronic mail: hhchang@mail.ndhu.edu.tw

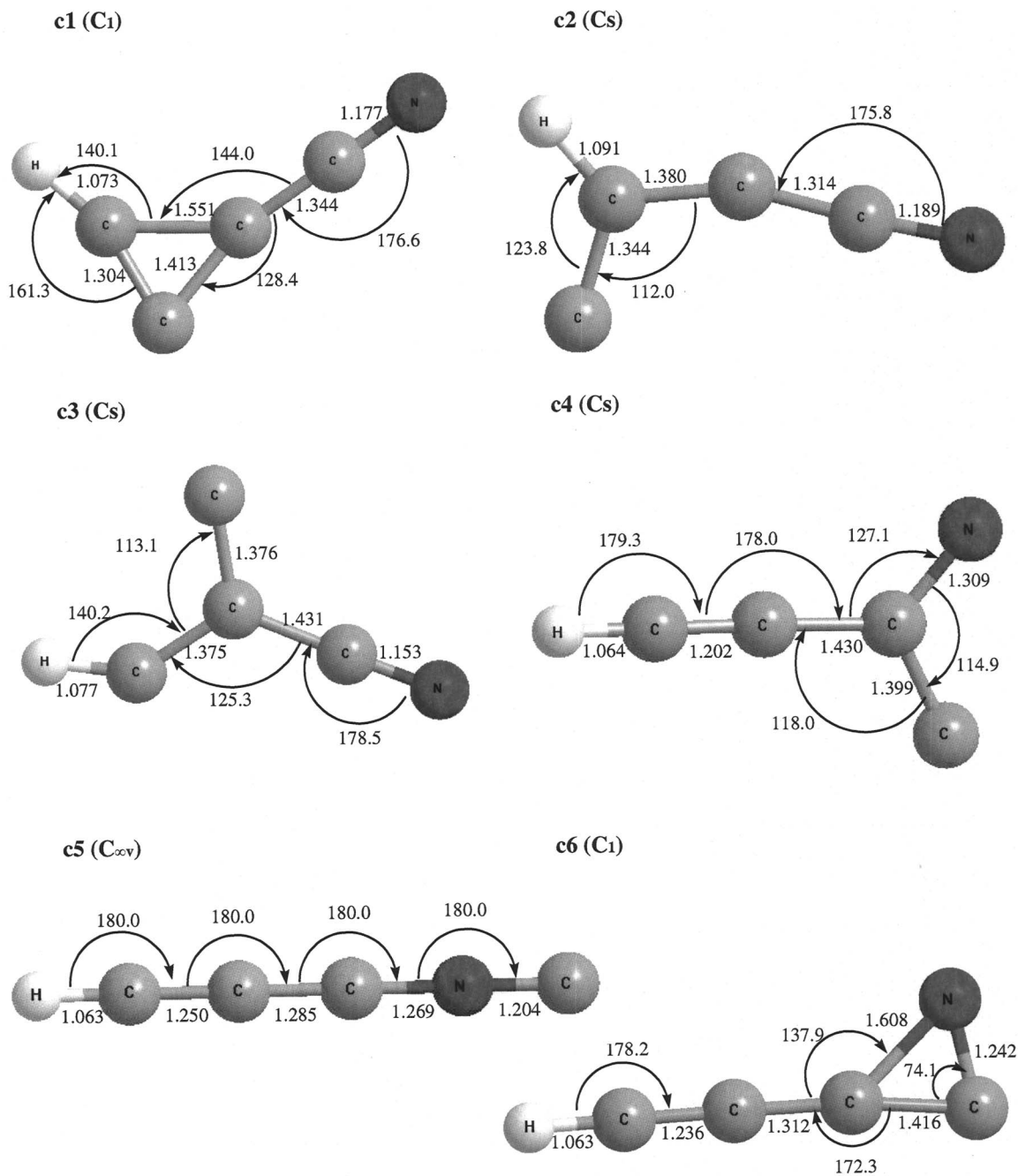


FIG. 1. The B3LYP/6-311G(*d,p*) optimized geometries of the six collision complexes of the $C(^3P)+HCCCN(X^1\Sigma^+)$ reaction, in which the point group is in parenthesis, lengths in angstrom, and the angles in degree.

through the addition to the carbon-carbon multiple bond or the triple bond of the cyano group, the carbon atom, abundant in the interstellar clouds, is expected to react readily with unsaturated nitriles, leading to the growth of versatile molecules by one more carbon unit.⁴² One of the most important and fascinating interstellar molecules that have been observed are the family of cyanopolyynes. Since the discovery of the simplest member cyanoacetylene (HCCCN) in 1971 by Turner,⁴³ widespread interest has been stirred; the linear carbon-chained cyanopolyynes, $HC_{2n+1}N$ ($n=1-5$), have all been detected in cold molecular clouds.⁴³⁻⁴⁶ The fate of HCCCN is believed to be crucial in synthesizing the more complex counterparts. Herbst *et al.*¹⁵

have incorporated the reaction $C+HCCCN\rightarrow C_4N+H$ to their chemical models of interstellar clouds, mainly as a depletion channel for cyanoacetylene. The results show a drastic effect on the abundances of cyanopolyynes, which signifies the potential importance of $C(^3P)+$ cyanopolyyne reaction; however, the details concerning its reaction channels, products, and dynamics have not been examined and remained unclear.

Theoretical study often holds the advantages in unveiling detailed reaction mechanism, in which the intermediates, transition states, and products that define reaction paths are characterized, while generally speaking only reactant consumptions or product formations are measured in the experi-

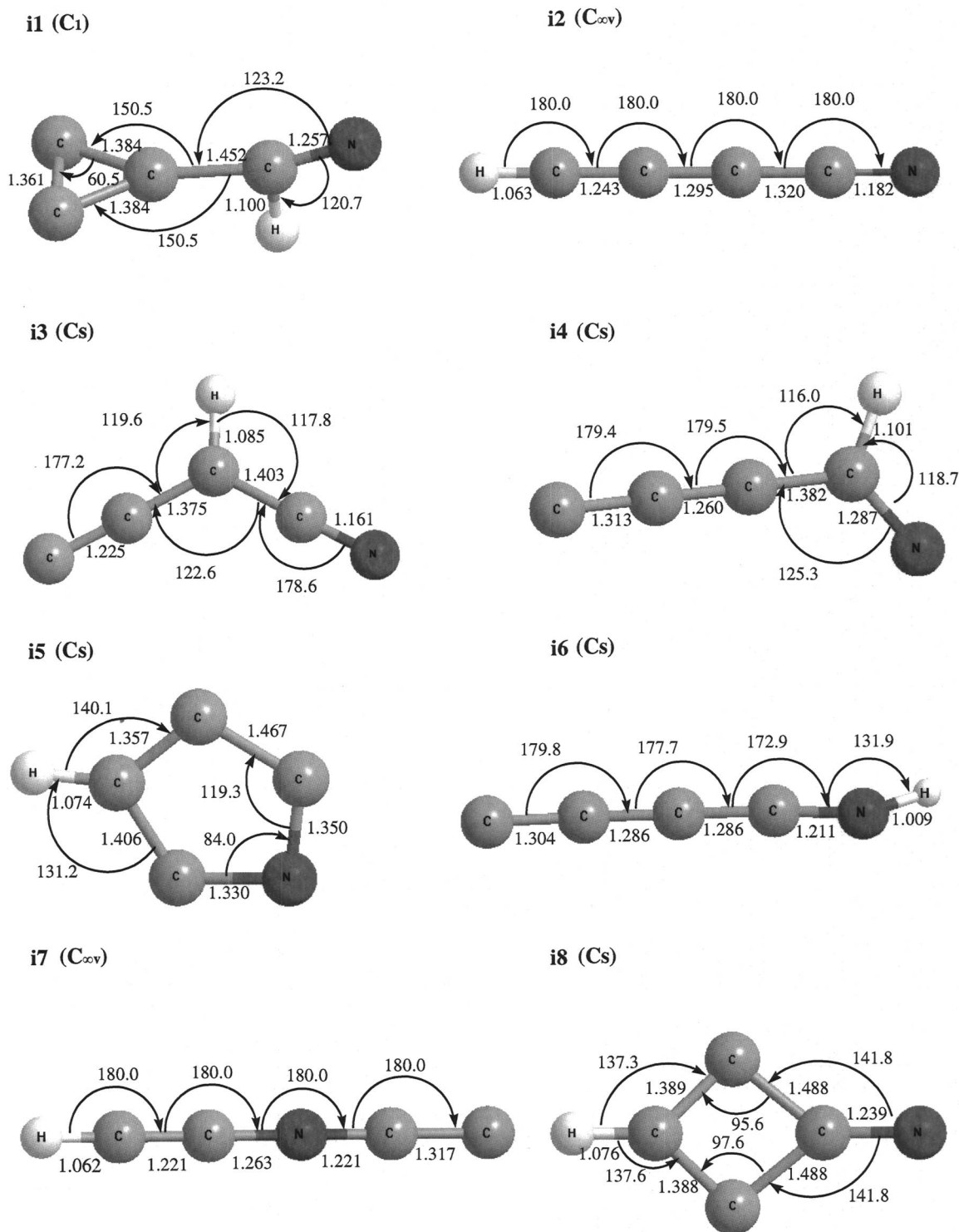


FIG. 2. The B3LYP/6-311G(*d,p*) optimized geometries of the intermediates for the $C(^3P)+HCCCN(X^1\Sigma^+)$ reaction on the adiabatic triplet-ground-state potential-energy surface of C_4HN , in which the point group is in parenthesis, the lengths in angstrom, and the angles in degree.

ments. The aim of the current theoretical investigation for the prototype $C(^3P)+HCCCN(X^1\Sigma^+)$ reaction is to identify the channels with no entrance barrier, which are relevant to the environments of ultralow temperature in interstellar clouds, to calculate the rate constants of elementary steps specifically tuned for single-collision condition, and to assess the product abundance.

It is worth noting that there are multiple π systems in cyanoacetylene molecule, which is expected to yield one of

multiple collision complexes when attacked by a carbon atom. The estimation for the bimolecular rate constant of a barrierless reaction has been known to be a challenging task, in particular, when it is orientation dependent and multidimensional as the titled reaction of six-atomic system. From a fundamental point of view, the present work could serve as an effort toward obtaining a multidimensional and orientation-dependent bimolecular rate constants for a barrierless reaction.

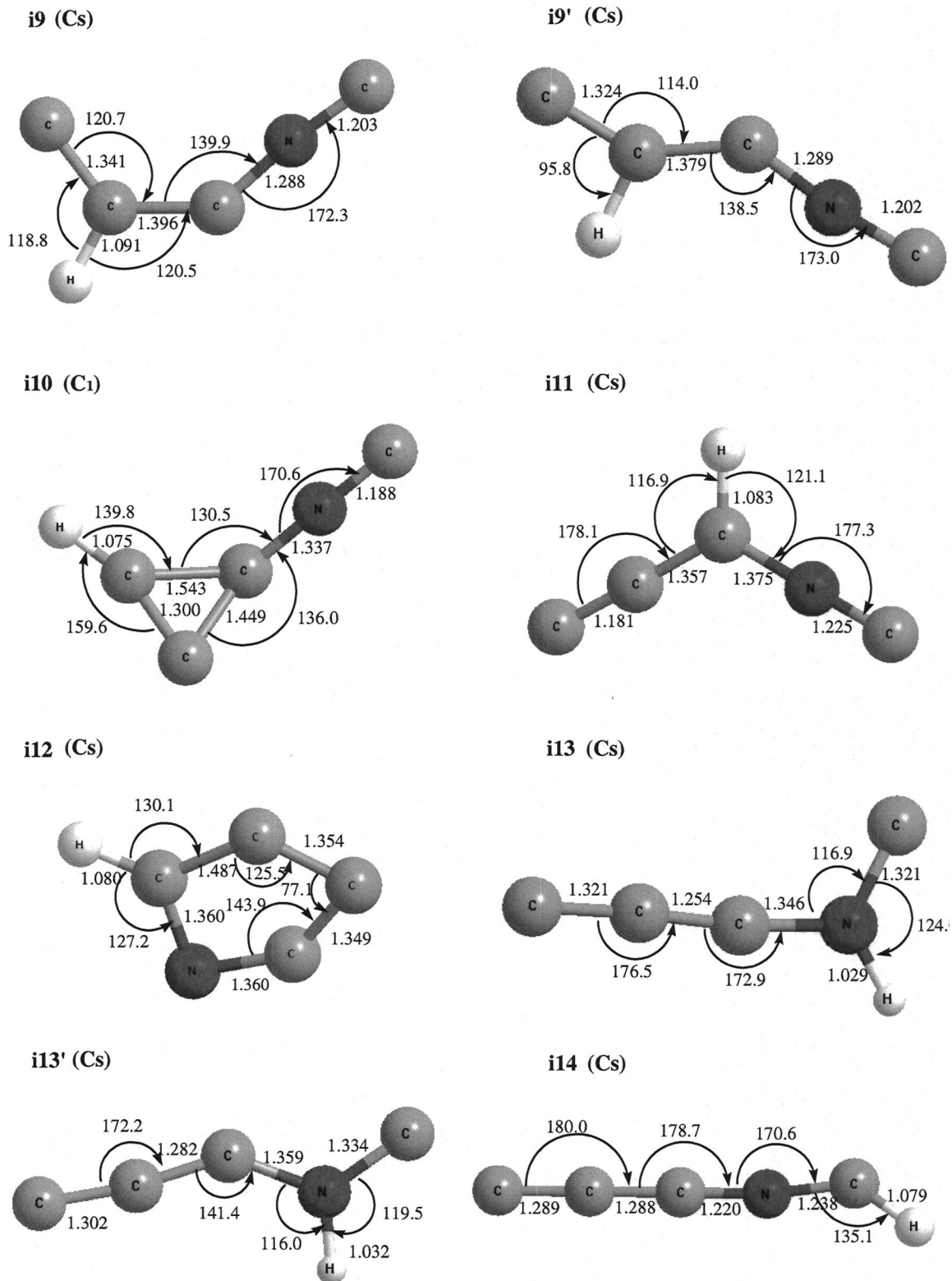


FIG. 2. (Continued).

II. THEORETICAL METHODS

A. *Ab initio* electronic structure calculations: Reaction path predictions

The $C(^3P)+HCCCN(X^1\Sigma^+)$ reaction is assumed to proceed adiabatically that the channels on the adiabatic triplet ground-state potential-energy surface of C_4HN are

investigated. The paths with energy below the reactants are emphasized since they would dominate in collision-induced reaction at ultralow temperature. The geometries and harmonic frequencies of intermediates, transition states, and dissociation products along the reaction paths are obtained at the level of the hybrid density-functional theory, the unre-

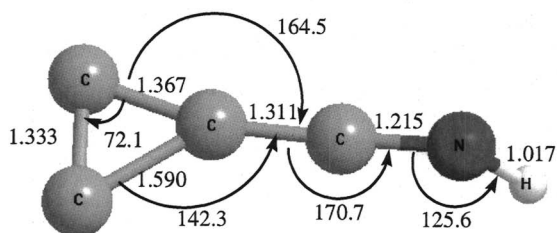
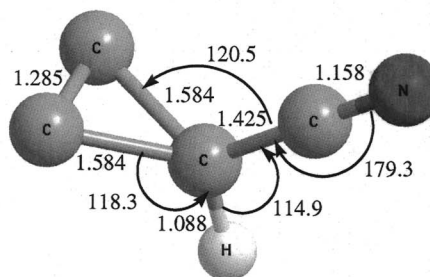
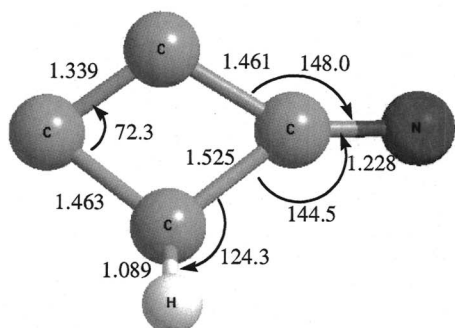
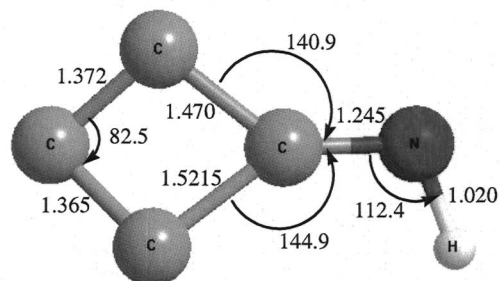
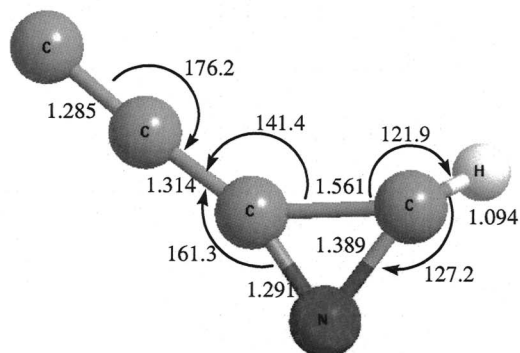
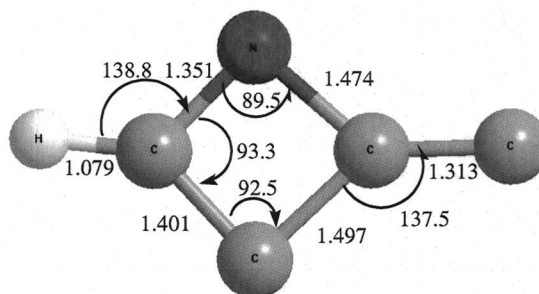
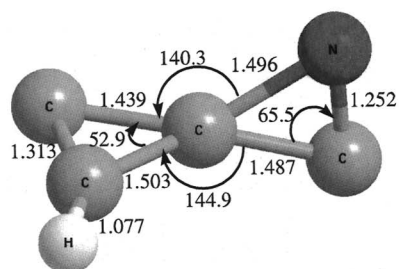
i15 (C₁)**i16 (C₁)****i17 (C₁)****i18 (C₁)****i19 (C₁)****i20 (C_s)****i21 (C₁)**

FIG. 2. (Continued).

stricted B3LYP/6-311G(*d,p*) (Ref. 47). For each species characterized, the energy is further refined by the coupled cluster⁴⁸ CCSD(T)/cc-pVTZ with B3LYP/6-311G(*d,p*) zero-point energy corrections. The GAUSSIAN 98 program⁴⁹ is utilized in the electronic structure calculations.

B. RRKM rate constant calculations

If the rate of the energy equilibration among degrees of freedom in the molecule is faster than the reaction rate, the rate constant can be explained statistically. Furthermore, in

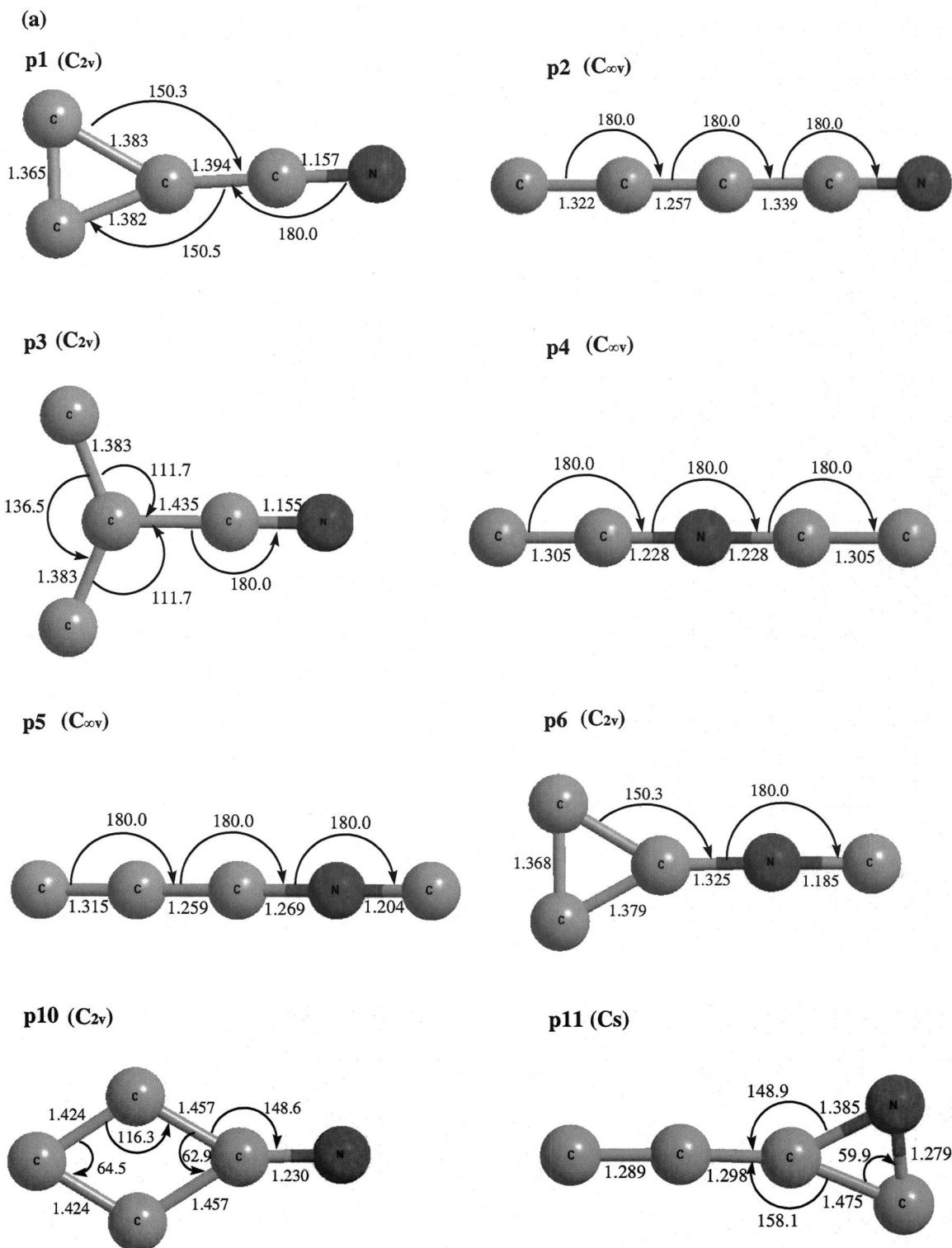


FIG. 3. The B3LYP/6-311G(*d,p*) optimized geometries of dissociation products for the $C(^3P)+HCCCN(X^1\Sigma^+)$ reaction, in which the point group is in parenthesis, the lengths in angstrom, and the angles in degree: (a) the hydrogen atom dissociation products, C_4N , in doublet ground states; (b) the CN dissociation products, C_3H , in doublet ground states. The structure of the linear p8 is optimized with unrestricted MP2/6-311G(*d,p*) calculations.

the environments such as interstellar clouds and crossed-beam experiments, the reaction proceeds with single collision and the energy is conserved throughout. Provided that both circumstances are met, the rate constant can be appropriately described by the Rice-Ramsperger-Kassel-Marcus

(RRKM) theory. Explicitly, in a unimolecular reaction $A^* \xrightarrow{k} A^\ddagger \rightarrow P$, where A^* is the energized reactant, A^\ddagger the transition state, and P is the products, the rate constant $k(E)$ as a function of energy is expressed as

(b)

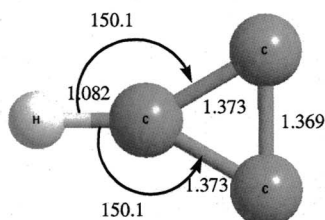
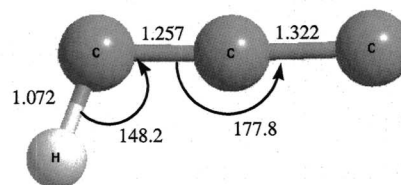
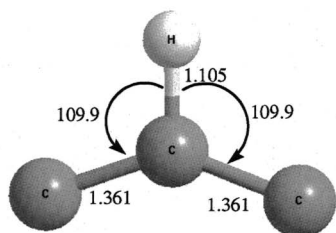
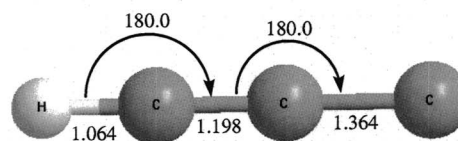
p7 (C_{2v})**p8** (C_s)**p9** (C_{2v}) $(C_{\infty v})$ 

FIG. 3. (Continued).

$$k(E) = \frac{\sigma W^\ddagger(E - E^\ddagger)}{h \rho(E)}, \quad (1)$$

where σ is the symmetry factor, W^\ddagger the number of states of the transition state, and ρ the density of states of the reactant. In this work, the saddle-point method^{50,51} is applied to evaluate the number of states and the density of states; the molecule is viewed as a collection of harmonic oscillators, of which the harmonic frequencies and energy are obtained as described in Sec. II A.

C. Variational RRKM rate constant calculations

The transition state is usually chosen as the geometry at the top of the reaction barrier or the saddle point, which poses a complication when the reaction is barrierless. For instance, as encountered at present work, the paths for the collision complexes dissociating back to the reactants, $C(^3P) + HCCCN$, are in fact barrierless. Alternatively, the geometry that minimizes the flux of trajectories is to assume the role of transition state. That is, the variational transition state is determined by the criterion (e.g., Refs. 52–54),

$$\frac{\partial W(E, R)}{\partial R} = 0, \quad (2)$$

where W is the number of states and R is the reaction coordinate, the breaking C–C or C–N bond in this work. Note the geometries of transition states thus located are both energy and reaction-coordinate dependent. The intrinsic reaction coordinate (IRC) calculations of optimized geometries and

corresponding harmonic frequencies as a function of the reaction coordinate for each collision complex are performed at the level of B3LYP/6-311G(*d,p*). Once the transition state is variationally decided for each collision complex at each of the six collision energies, its corresponding CCSD(T)/cc-pVTZ energy is computed and the rate constant $k(E)$ of the unimolecular reaction could be calculated according to the RRKM theory in Eq. (1).

III. RESULTS AND DISCUSSIONS

As a result of electron deficient $C(^3P)$ attacking the π -electron systems of HCCCN, six possible collision complexes (c1–c6) seen in Fig. 1 are located with B3LYP/6-311G(*d,p*) calculations. c1, c2, and c3 are formed by carbon addition to carbon-carbon triple bond; when the addition is to the cyano group, it gives c4, c5, and c6.

The species produced due to isomerization of the collision complexes, which includes hydrogen migration, carbon migration, ring opening, ring closing, and rotation, are denoted as *i* whose optimized geometries are displayed in Fig. 2. The geometries of the hydrogen and cyano dissociation products designated as *p* are shown in Fig. 3. The transition state (ts) structures are depicted in Fig. s1,⁵⁵ and the variational transition states, tsc1, tsc2, tsc3, tsc4, tsc5, and tsc6, for the reversed reactions of c1, c2, c3, c4, c5, and c6 back to $C + HCCCN$, respectively, are illustrated in Fig. 4. The B3LYP/6-311G(*d,p*) and CCSD(T)/cc-pVTZ energies for all the species investigated are tabulated in Table s1.⁵⁵ The channels for complexes c1–c6 are illustrated in Figs. 5–10, respectively, where the energies relative to the reactants, $C(^3P) + HCCCN(X^1\Sigma^+)$, at CCSD(T)/cc-pVTZ level of

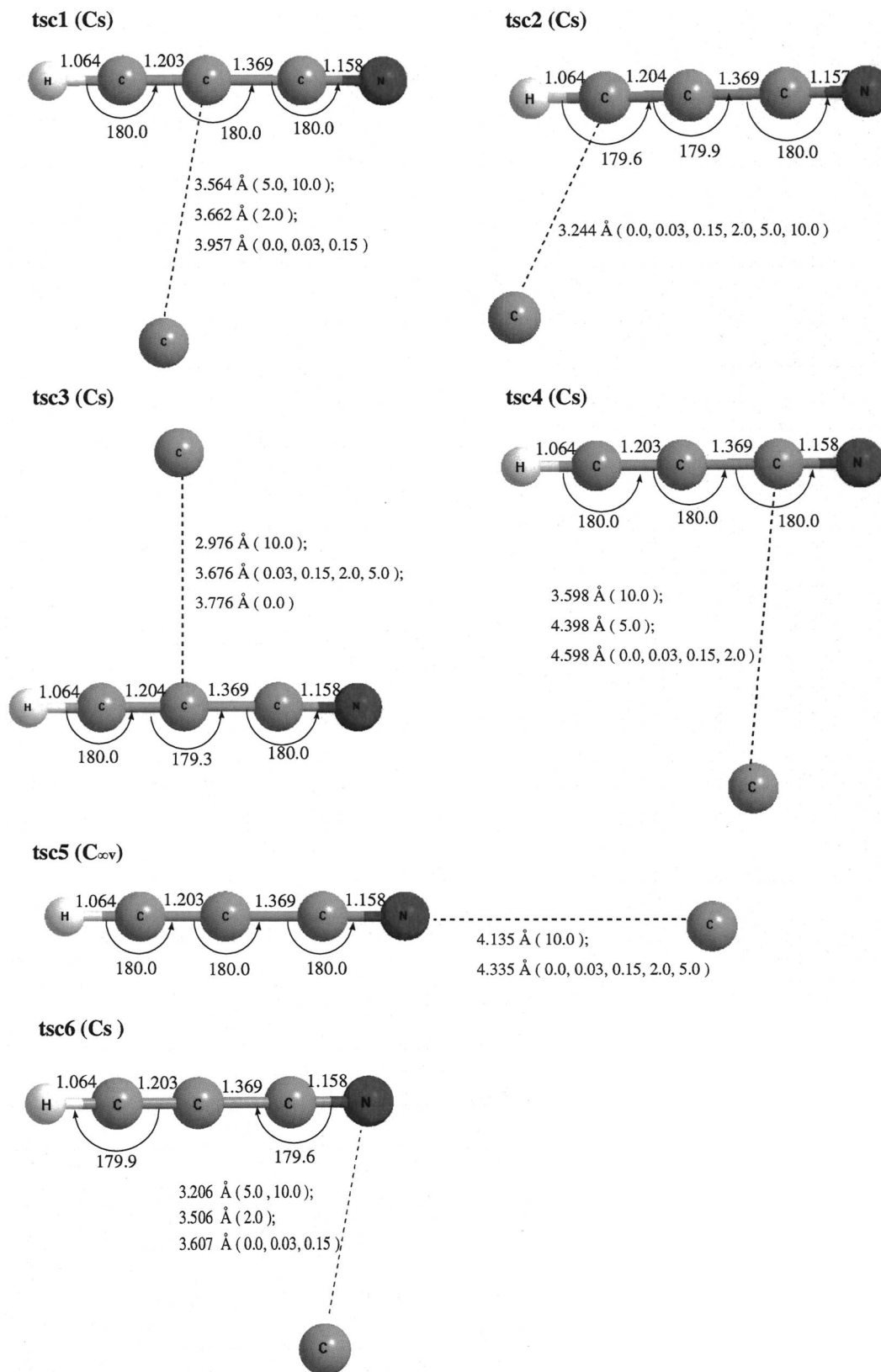


FIG. 4. The schematic B3LYP/6-311G(*d,p*) geometries of variational transition states for carbon decomposition reactions of collision complexes, c1–c6, on the adiabatic triplet-ground-state potential-energy surface of C₄HN, in which the point group is in parenthesis, the lengths in angstrom, and the angles in degree. Also note that the collision energies are specified in the parentheses next to the corresponding breaking CC bond lengths of tsc1–tsc4, and CN bond lengths of tsc5 and tsc6.

theory are cited, and only the reactions of the isomers along the minimum energy path are traced further to pin down the major products unless otherwise stated. The rate constants

based on the RRKM and variational RRKM theories for important elementary steps at collision energies, 0.0, 0.03, 0.15, 2.0, 5, and 10 kcal/mol, are listed in Table I, which corre-

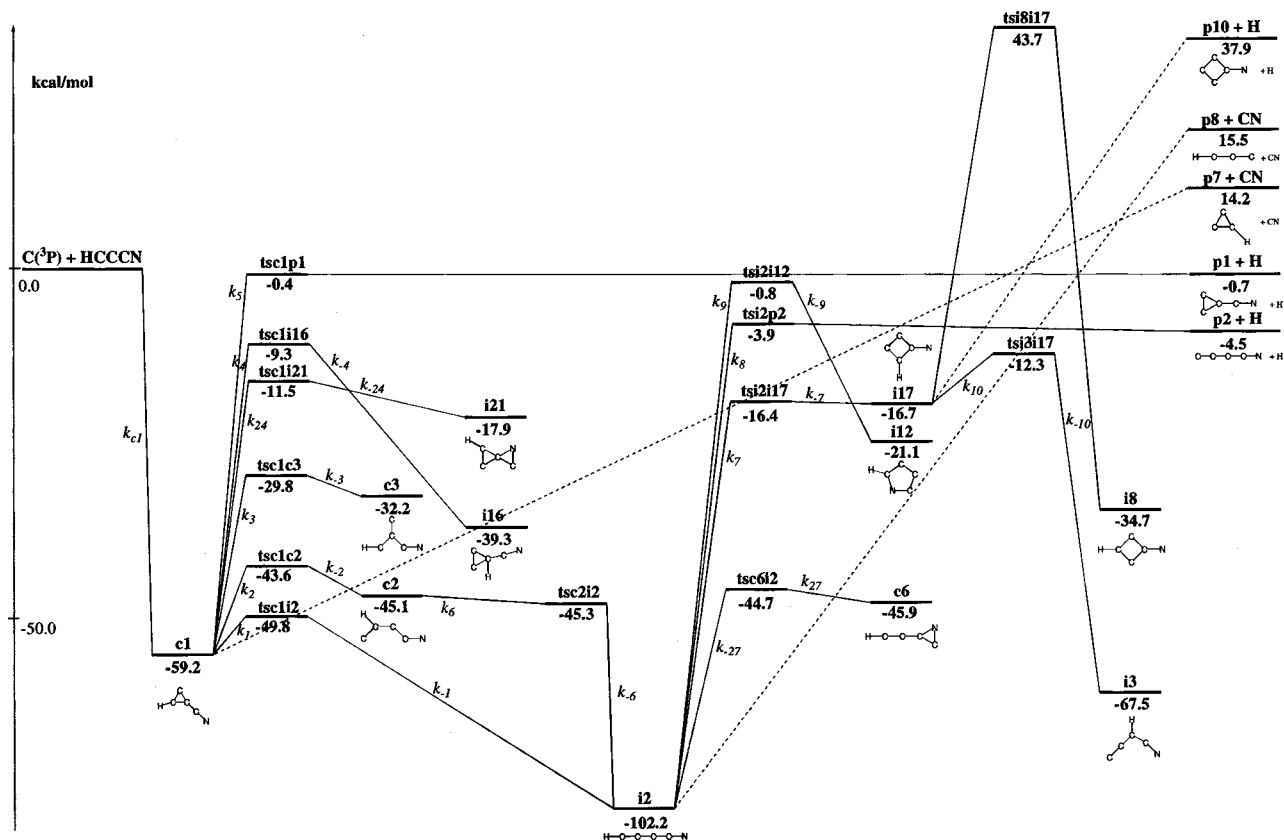


FIG. 5. The reaction paths of the collision complex, $c1$, in which the energies in kcal/mol relative to the reactants, $C(^3P) + HCCCN(X^1\Sigma^+)$, are computed with CCSD(T)/cc-pVTZ level of theory with B3LYP/6-311G(d,p) zero-point energy corrections at the B3LYP/6-311G(d,p) optimized geometries, as shown in Figs. 1–4. Note the attempts are not made to locate the transition states for those paths in dotted lines.

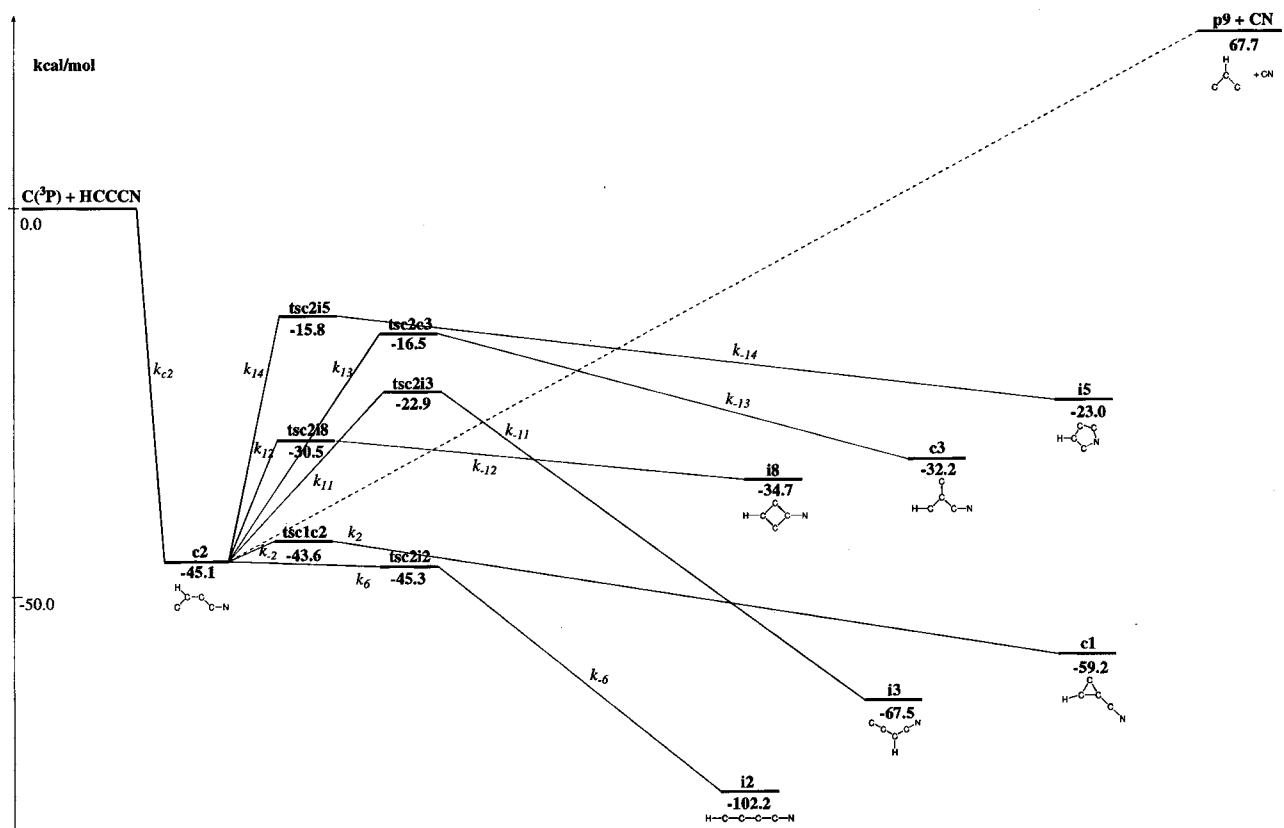


FIG. 6. The reaction paths of the collision complex, $c2$, in which the energies in kcal/mol relative to the reactants, $C(^3P) + HCCCN(X^1\Sigma^+)$, are computed with CCSD(T)/cc-pVTZ level of theory with B3LYP/6-311G(d,p) zero-point energy corrections at the B3LYP/6-311G(d,p) optimized geometries as shown in Figs. 1–4. Note the attempts are not made to locate the transition states for those paths in dotted lines.

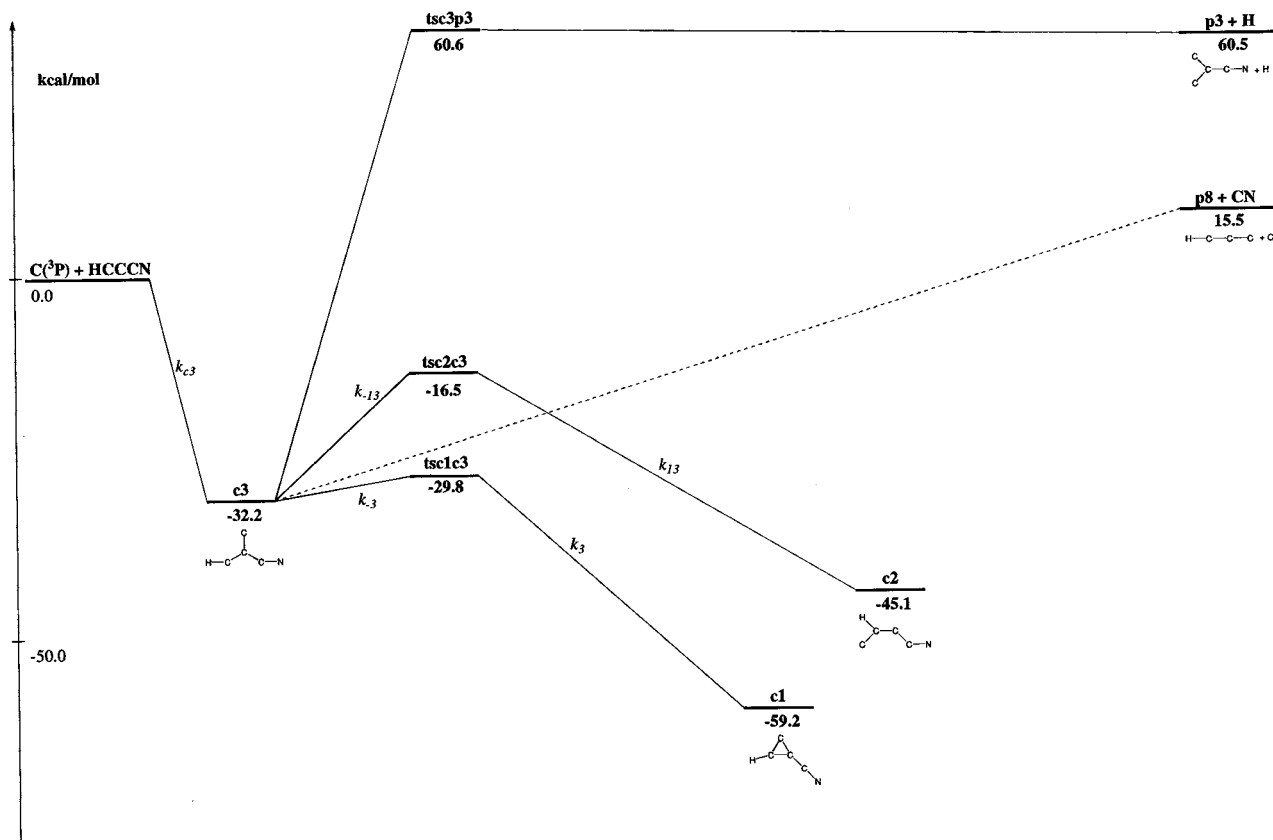


FIG. 7. The reaction paths of the collision complex, c_3 , in which the energies in kcal/mol relative to the reactants, $C(^3P) + HCCCN(X^1\Sigma^+)$, are computed with CCSD(T)/cc-pVTZ level of theory with B3LYP/6-311G(*d,p*) zero-point energy corrections at the B3LYP/6-311G(*d,p*) optimized geometries, as shown in Figs. 1–4. Note the attempts are not made to locate the transition states for those paths in dotted lines.

spond to the average kinetic energies of an ideal-gas molecule at temperatures of 0, 10, 50, 671, 1678, and 3355 K, respectively.

A. H and CN dissociation products

As shown in Table sI, among isomers produced from the dissociation of hydrogen atom and cyano radical, only H-dissociation products of C–C–C three-member-ringed cycloprop-1,2,3-triene nitrile (p1) and the linear but-1,2,3-triene-4-ylidene nitrile (p2) are energetically accessible at 0.0 collision energy or ultralow temperature. p2+H is the most stable products, with a CCSD(T)/cc-pVTZ energy of -4.5 kcal/mol with respect to the reactants. The most stable isomer of the famed C_3H molecule,⁵⁶ cyclic p7, is reachable by at least 14.2 kcal/mol above the reactants.

B. Dissociation of collision complexes back to reactants, C+HCCCN

Determined by variational RRKM theory at six collision energies, 0.0, 0.03, 0.15, 2, 5, and 10 kcal/mol, the total 36 transition states (tsc1–tsc6) for c1–c6 dissociating back to C+HCCCN are shown in Fig. 4 with corresponding energies listed in Table sI. Generally speaking, the bond lengths for the breaking C–C bonds in tsc1–tsc4 and C–N bonds in tsc5 and tsc6 decrease as the collision energy increases, or the transition states are tighter; the activation energy also decreases with increasing collision energy. As indicated in

Table sI, since the energies of tsc1–tsc6 are similar, the magnitudes of the rate constants would largely depend on the energy of collision complexes. Specifically, the more stable the collision complex, the higher the barrier for dissociation back to reactants is. The collision complexes are predicted to have an energetic order of $c_5 < c_1 < c_6 < c_2 < c_3 < c_4$; accordingly in Table I, the rate constants indeed follow the similar trend: $k_{c_5} < k_{c_1} \sim k_{c_6} < k_{c_2} < k_{c_3} < k_{c_4}$, with comparable k_{c_1} and k_{c_6} due to a tighter c_6 than c_1 .

The variational transition state for a barrierless reaction is typically of energy lower than the final products, which in this case are C+HCCCN. For instance, at 0.0 collision energy, the transition states tsc1–tsc6 are located within -6.9 – -7.3 kcal/mol, which is nevertheless notably lower than the -4.5 kcal/mol of the lowest dissociation products, p2+H. The scenario raises an intriguing question: will the collision complexes decompose back to the reactants so that the C+HCCCN reaction appears not reactive, or they lose a hydrogen atom to generate a new species, or both? Although the energetic factor seems to favor the reproduction of reactants over the hydrogen-atom dissociation, kinetically it may prove otherwise, especially for c1–c3, c5, and c6, as discussed in the following sections.

C. Reaction paths of cyclopropa-1,2-diene nitrile (c1)

c1 could isomerize via ring opening, ring closing, and 1,2 H shift: the former gives but-1,2-diene-3-yne nitrile (i2), c2, and c3, while a biringed aziridine-1-ene-3-yl-ylidene-

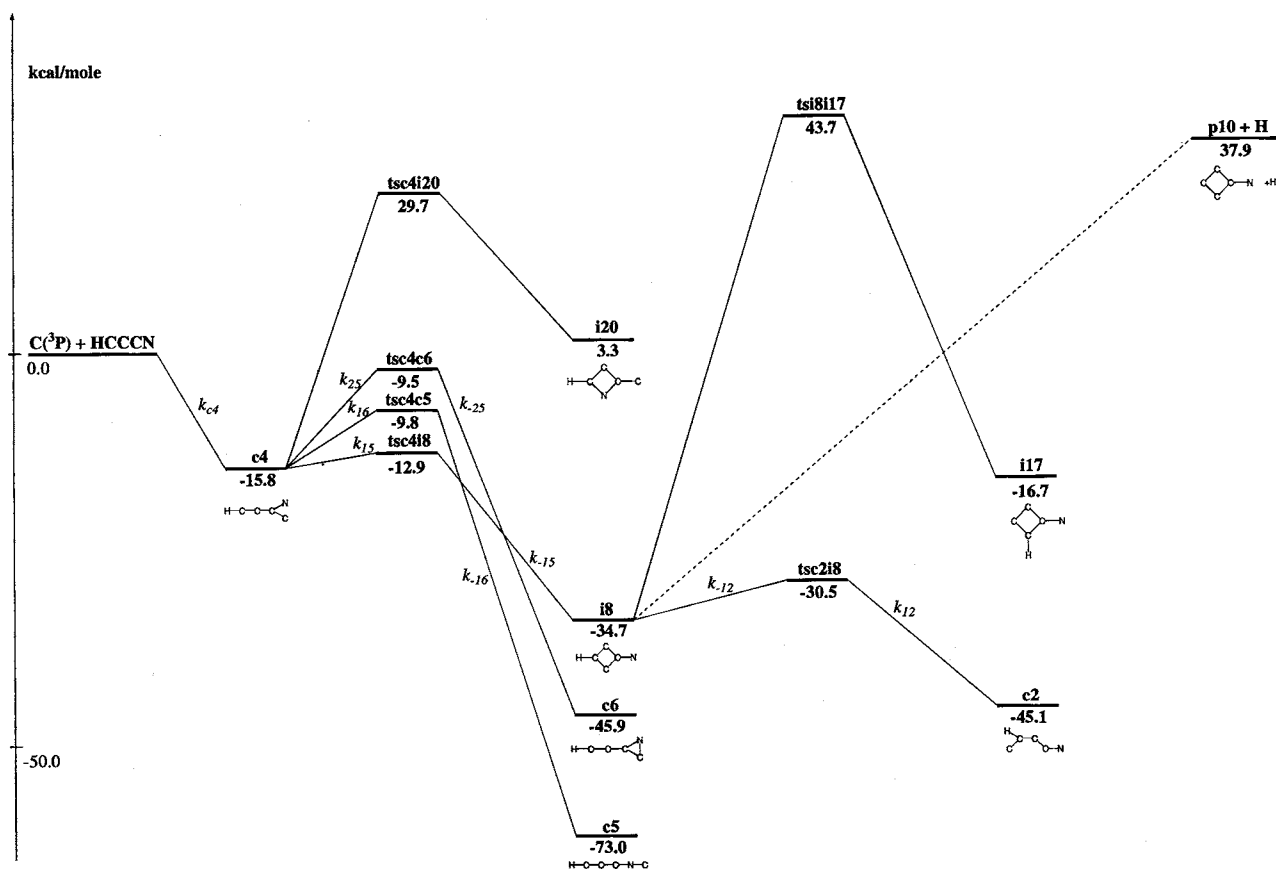


FIG. 8. The reaction paths of the collision complex, c_4 , in which the energies in kcal/mol relative to the reactants, $C(^3P) + HCCCN(X^1\Sigma^+)$, are computed with CCSD(T)/cc-pVTZ level of theory with B3LYP/6-311G(d,p) zero-point energy corrections at the B3LYP/6-311G(d,p) optimized geometries, as shown in Figs. 1–4. Note the attempts are not made to locate the transition states for those paths in dotted lines.

ethene (i_{21}) is formed as a result of the latter and the latest takes c_1 to 3-cyano cyclopropen-1,2-diyl (i_{16}); hydrogen-atom dissociation of c_1 generates $p_1 + H$ of CCSD(T)/cc-pVTZ energy of -0.7 kcal/mol and the carbon decomposition brings c_1 back to the reactants. All seven channels are energetically below the reactants $C(^3P) + HCCCN$. As seen in Table S1 and Fig. 5, the c_1 ring opening yielding the most stable isomer i_2 requires the least of activation energy, predicted to be 9.4 kcal/mol by CCSD(T)/cc-pVTZ, compared to the second least hindered route, $c_1 \rightarrow c_2$, with a barrier of 15.6 kcal/mol. It makes the $c_1 \rightarrow i_2$ reaction most likely to occur, which is also confirmed by the rate constant calculations. Except for $k_{c_1}(c_1 \rightarrow C + HCCCN)$, which has a particularly loose transition state and thus is estimated larger than its barrier would suggest, the magnitudes of the rest of 5 RRKM rate constants decrease with increase of the corresponding activation energy: at collision energy of 0.0 kcal/mol, $k_1(c_1 \rightarrow i_2)$, $k_2(c_1 \rightarrow c_2)$, $k_3(c_1 \rightarrow c_3)$, $k_{24}(c_1 \rightarrow i_{21})$, $k_4(c_1 \rightarrow i_{16})$, and $k_5(c_1 \rightarrow p_1 + H)$ are computed to be 3.58×10^{12} , 9.62×10^{11} , 1.92×10^{10} , 3.17×10^7 , 1.04×10^7 , and 1.40×10^4 s^{-1} , respectively. It is easily seen that the rate constant for the third fastest channel, $c_1 \rightarrow c_3$, k_3 , already trails behind k_1 by a factor of 180, and that the decomposition either to $C + HCCCN$ or to cyclic $p_1 + H$ is decidedly negligible.

The calculations indicate that there are seven channels

open for i_2 : the 1,2 H shift to c_2 , ring closures to c_1 , c_6 of three-membered ring, i_{17} of four-membered ring, five-membered-ringed azacyclopent-1,2,3-triene-4,5-diyl (i_{12}), hydrogen atom and cyano radical dissociations to but-1,2,3-triene-4-ylidene nitrile (p_2) + H, and propdiene-1-yl-3-ylidene (p_8) + CN, respectively. With the exception of $p_8 + CN$, which is computed to have energy at 15.5 kcal/mol, all other six reaction paths are bound relative to the reactants. Interestingly, it appears that i_2 is in fact the most likely destination for its four immediate intermediates requiring the lowest activation energies, c_2 , c_1 , c_6 , and i_{17} , once they are formed. The channels for c_2 and c_6 are discussed in the sections that follow. Only two of the four possible ring-opening reactions of i_{17} are characterized, which give i_2 and cyanovinylidene carbene (i_3); hydrogen migration in i_{17} yields i_8 ; its products of direct hydrogen loss, $p_{10} + H$, are also found. Among those, i_{17} back to i_2 encounters virtually no barrier. Thus, the buildup of i_2 is inevitable unless the irreversible leaking to dissociation products, $p_2 + H$ or $p_8 + CN$, is accessible. The latter would not be feasible at ultralow temperature. Even though $k_8(i_2 \rightarrow p_2 + H)$, being 2.57×10^4 s^{-1} , is much less than $k_{-1}(i_2 \rightarrow c_1)$, $k_{-6}(i_2 \rightarrow c_2)$, and $k_{-27}(i_2 \rightarrow c_6)$, evaluated to be 1.50×10^9 , 3.40×10^8 , and 9.63×10^8 s^{-1} , respectively, with tsi_{2p_2} located at -3.9 kcal/mol, neither kinetically nor energetically favored $p_2 + H$ would become the destination of i_2 .

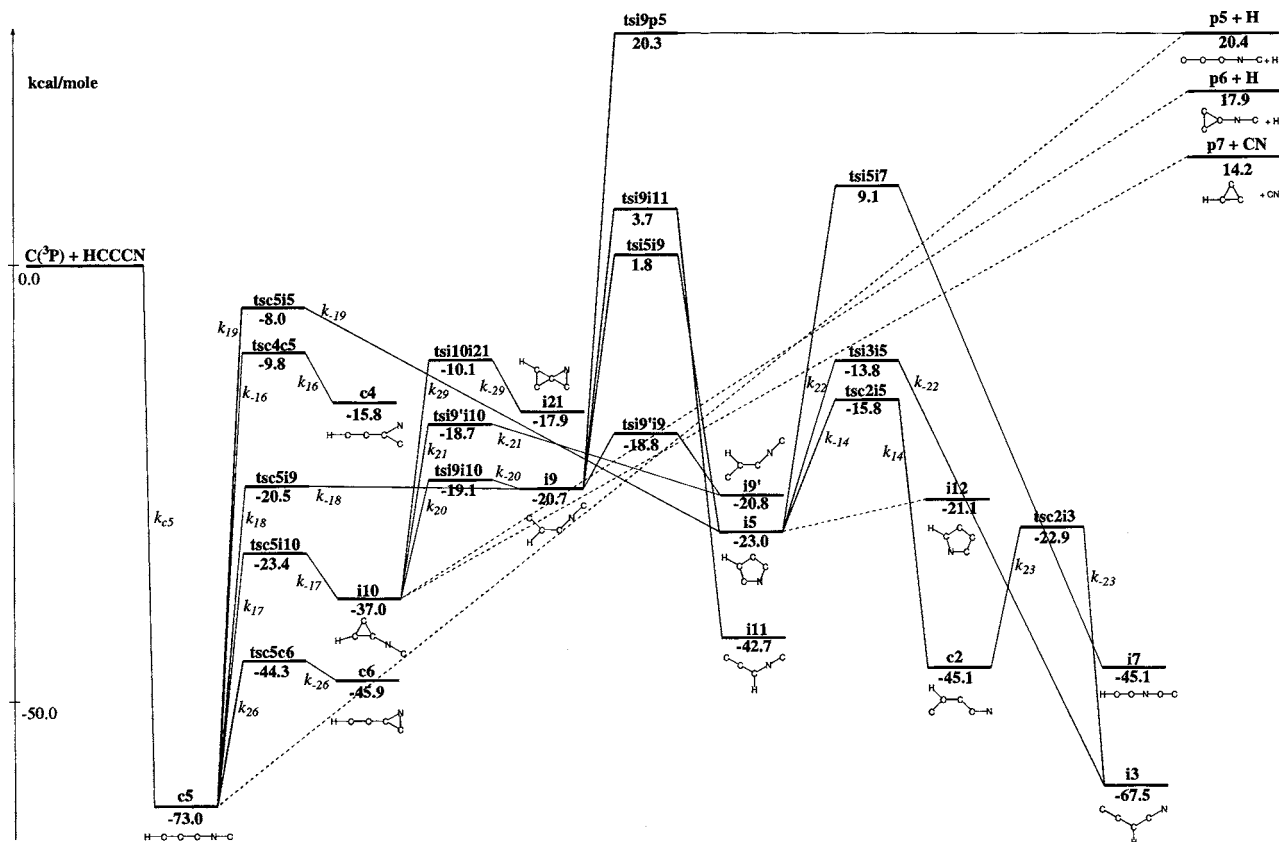


FIG. 9. The reaction paths of the collision complex, c_5 , in which the energies in kcal/mol relative to the reactants, $C(^3P) + HCCCN(X^1\Sigma^+)$, are computed with CCSD(T)/cc-pVTZ level of theory with B3LYP/6-311G(*d,p*) zero-point energy corrections at the B3LYP/6-311G(*d,p*) optimized geometries, as shown in Figs. 1–4. Note the attempts are not made to locate the transition states for those paths in dotted lines.

D. Reaction paths of but-3-ene-4,4-diyl-1-yne nitrile (c_2)

c_2 reaction paths in Fig. 6 reveal that the transition states for three-, four-, and five-membered ring closures of c_2 resulting in c_1 , i_8 , and azacyclopent-3,5-diene-3,5-diyl (i_5), respectively, have been found; c_2 could also undergo C migration to become complex c_3 ; 1,2 H shift leads c_2 to i_2 and cyano 1-propen-2-yne-3-yl (i_3). Both 1,3 H shift and 1,3-C shift of c_2 to cyano but-1,2,3-triene-4,4-diyl (i_4) and c_4 , respectively, seem unlikely, since the transition states could not be located despite various attempts; likewise, the c_2 H dissociation to the obvious products of $p_2 + H$ also appears not probable.

Similar to c_1 , the most probable path of c_2 would easily be the one leading to i_2 , either directly or via c_1 . The CCSD(T)/cc-pVTZ energy predicted for tsc_{2i2} is -45.3 kcal/mol, slightly lower than the -45.1 kcal/mol of c_2 , an indication of c_2 being highly unstable with respect to the H migration to i_2 . The second most competitive channel, $c_2 \rightarrow c_1$, is not far behind with the energy of tsc_{1c2} being -43.6 kcal/mol. The rate of $c_2 \rightarrow i_2$ reaction must be extraordinarily fast knowing that the $k_{-2}(c_2 \rightarrow c_1)$ is already $8.56 \times 10^{12} \text{ s}^{-1}$ at 0.0 collision energy.

E. Reaction paths of 2-cyano-allene-a-al-3-ylidene (c_3)

As shown in Fig. 7, the options for c_3 are predicted to be rather limited compared with c_1 and c_2 . Only the channels of

reversed reaction to $C + HCCCN$, cyclization to c_1 , carbon migration to c_2 , and hydrogen-dissociation to 2-cyano-propadiene-diylidene (p_3) + H could be characterized, among which the minimum energy path, $c_3 \rightarrow c_1$, easily dominates owing to its much lower barrier of 2.4 kcal/mol. The rate constant calculations estimate $k_{-3}(c_3 \rightarrow c_1)$ to be $7.16 \times 10^{11} \text{ s}^{-1}$ at 0.0 collision energy, around 44 times larger than the next energetically and kinetically favored $k_{-13}(c_3 \rightarrow c_2)$ of $1.62 \times 10^{10} \text{ s}^{-1}$. Therefore, the paths of c_1 are expected to follow afterward, as discussed in Sec. III C. Efforts in locating the paths to other carbon-migration route, four-membered ring closures, H shift, and CN shift have also been made, however, without success.

F. Reaction paths of c_4

For the least stable collision complex, c_4 , with tsc_4 found at CCSD(T)/cc-pVTZ energy of -7.2 kcal/mol at 0.0 collision energy, its decomposition back to the reactants is a serious contender among probable isomerization reactions. The species resulted from direct H loss in c_4 has not been located at present level of calculations, and the channel of N shifting to i_2 is also not found. Four other options are open for c_4 , as seen in Fig. 8. Namely, three-membered ring (CNC) formation gives c_6 , four-membered ring closure converts c_4 to i_8 and i_{20} , and C shift brings c_4 to c_5 , with barriers predicted to be 6.3, 2.9, 45.5, and 6.0 kcal/mol, respectively.

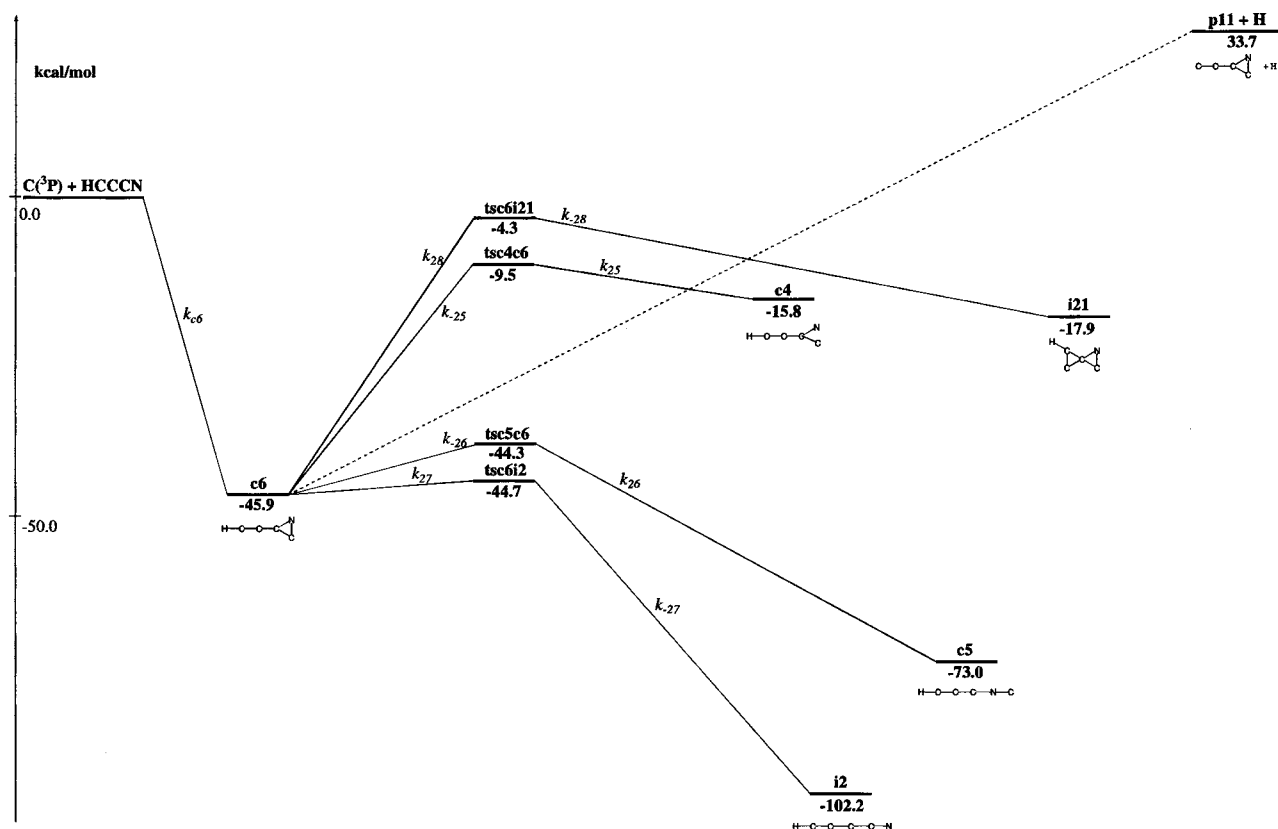


FIG. 10. The reaction paths of the collision complex, c_6 , in which the energies in kcal/mol relative to the reactants, $C(^3P) + HCCCN(X^1\Sigma^+)$, are computed with CCSD(T)/cc-pVTZ level of theory with B3LYP/6-311G(d,p) zero-point energy corrections at the B3LYP/6-311G(d,p) optimized geometries, as shown in Figs. 1–4. Note the attempts are not made to locate the transition states for those paths in dotted lines.

In spite of a higher activation energy, k_{c_4} is nonetheless 2.5–6.5 times faster than $k_{15}(c_4 \rightarrow i_8)$ as the collision energy increases from 0.0 to 10.0 kcal/mol. For collision energy in the range of 0.0–5.0 kcal/mol, k_{15} and $k_{16}(c_4 \rightarrow c_5)$ are comparable with the former keeping a slight winning edge consistent with the heights of their barriers. When the collision energy increases to 10 kcal/mol, k_{16} overtakes k_{15} as the second most favored. Being around 3/5 of k_{16} , the fourth largest rate constant, $k_{25}(c_4 \rightarrow c_6)$, is not far behind. The fates of c_5 and c_6 are discussed in the next sections. By overcoming an activation energy of mere 4.2 kcal/mol, i_8 could ring open to c_2 , while the 1,2 H shift bringing i_8 to i_{17} and direct H dissociation yielding $p_{10} + H$ are both consuming much costly barriers and thus much less significant. That is, if through intermediate i_8 , c_4 then proceeds as c_2 .

G. Reaction paths of isocyano-propa-1-yne-3-ylidene (c_5)

As illustrated in Fig. 9, the probable immediate paths of the most stable collision complex c_5 are identified to be three-(CNC and CCC) and five-membered ring closures, 1,2 H shift, 1,2 C shift, and the dissociation of a carbon atom, which generate c_6 , isocyano cycloprop-2-ene-1,2-diyl (i_{10}), i_5 , isocyano 1-propene-2-ene-3,3-diyl (i_9), c_4 , and

$C + HCCCN$, respectively. The possible products of c_5 H decomposition, isocyano propdiene-1-yl-3-ylidene (p_5) + H, are at a much higher energy of 20.4 kcal/mol. The CNC ring-closing $c_5 \rightarrow c_6$ reaction would be the apparent preferred route with an activation energy being 28.7 kcal/mol and the corresponding $k_{26} 1.92 \times 10^8 \text{ s}^{-1}$ at 0.0 collision energy. With a barrier of 49.6 kcal/mol, the channel of $c_5 \rightarrow i_{10}$ is the next energetically favored, and the $c_5 \rightarrow i_9$ reaction is predicted to be a close third with an activation energy of 2.9 kcal/mol higher. $k_{17}(c_5 \rightarrow i_{10})$ and $k_{18}(c_5 \rightarrow i_9)$ are evaluated to be 2.02×10^6 and $5.03 \times 10^5 \text{ s}^{-1}$, respectively, at 0.0 collision energy.

Among the probable channels found for i_9 , 1,2 H shift back to c_5 , three-membered ring closure to i_{10} , rotation to its *trans* counterpart i_9' , five-membered ring closure to i_5 , 1,2 H shift to isocyano 1-propene-2-yne-yl (i_{11}), and the H dissociation to $p_5 + H$, the path of $i_9 \rightarrow c_5$ encounters the least hindrance. Similarly for i_{10} , conversion to c_5 is also the minimum energy path when compared with the ring opening to i_9 and i_9' , the CNC ring closing to i_{21} , and possible dissociations to $p_7 + CN$ and cycloprop-1,2,3-triene isonitrile (p_6) + H. Note the four-membered and three-membered CNC ring formations of i_9 do not seem likely at B3LYP/6-311G(d,p) level of calculations, neither does the third possible ring opening for i_{10} .

In another words, i_9 and i_{10} convert back to c_5 instantly with rather large rate constants, $k_{-18}(i_9 \rightarrow c_5) = 9.35 \times 10^{12} \text{ s}^{-1}$ and $k_{-17}(i_{10} \rightarrow c_5) = 2.03 \times 10^{12} \text{ s}^{-1}$, even at 0.0

TABLE I. The RRKM rate constants (s^{-1}) computed with B3LYP/6-311G(*d,p*) zero-point energy-corrected CCSD(T)/cc-pVTZ energies, and B3LYP/6-311G(*d,p*) harmonic frequencies at collision energies of 0.0, 0.03, 0.15, 2.0, 5.0, and 10.0 kcal/mol.

	0.0	0.03	0.15	2.0	5.0	10.0
k_{c1} (c1 \rightarrow C+HCCCN)	6.80×10^7	6.92×10^7	7.39×10^7	7.35×10^7	1.92×10^8	8.31×10^8
k_{c2} (c2 \rightarrow C+HCCCN)	1.46×10^8	1.48×10^8	1.57×10^8	3.63×10^8	1.07×10^9	4.07×10^9
k_{c3} (c3 \rightarrow C+HCCCN)	1.16×10^9	1.01×10^9	1.06×10^9	2.26×10^9	5.84×10^9	1.40×10^{10}
k_{c4} (c4 \rightarrow C+HCCCN)	1.90×10^{12}	1.92×10^{12}	1.99×10^{12}	3.23×10^{12}	4.97×10^{12}	7.35×10^{12}
k_{c5} (c5 \rightarrow C+HCCCN)	9.29×10^3	9.44×10^3	1.01×10^4	2.54×10^4	2.90×10^4	1.33×10^5
k_{c6} (c6 \rightarrow C+HCCCN)	6.48×10^7	6.58×10^7	6.98×10^7	1.47×10^8	3.24×10^8	1.16×10^9
k_1 (c1 \rightarrow i2)	3.58×10^{12}	3.59×10^{12}	3.60×10^{12}	3.76×10^{12}	4.02×10^{12}	4.44×10^{12}
k_{-1} (i2 \rightarrow c1)	1.50×10^9	1.51×10^9	1.52×10^9	1.72×10^9	2.09×10^9	2.79×10^9
k_2 (c1 \rightarrow c2)	9.62×10^{11}	9.63×10^{11}	9.68×10^{11}	1.05×10^{12}	1.17×10^{12}	1.39×10^{12}
k_{-2} (c2 \rightarrow c1)	8.56×10^{12}	8.56×10^{12}	8.57×10^{12}	8.66×10^{12}	8.81×10^{12}	9.03×10^{12}
k_3 (c1 \rightarrow c3)	1.92×10^{10}	1.93×10^{10}	1.95×10^{10}	2.36×10^{10}	3.13×10^{10}	4.70×10^{10}
k_{-3} (c3 \rightarrow c1)	7.16×10^{11}	7.16×10^{11}	7.17×10^{11}	7.34×10^{11}	7.59×10^{11}	7.95×10^{11}
k_4 (c1 \rightarrow i16)	1.04×10^7	1.05×10^7	1.10×10^7	2.21×10^7	5.73×10^7	2.02×10^8
k_{-4} (i16 \rightarrow c1)	5.48×10^9	5.54×10^9	5.78×10^9	1.06×10^{10}	2.39×10^{10}	6.87×10^{10}
k_5 (c1 \rightarrow p1+H)	1.40×10^4	1.55×10^4	2.24×10^4	6.81×10^5	1.32×10^7	2.53×10^8
k_6 (c2 \rightarrow i2)
k_{-6} (i2 \rightarrow c2)	3.40×10^8	3.41×10^8	3.44×10^8	4.00×10^8	5.03×10^8	7.10×10^9
k_7 (i2 \rightarrow i17)	2.99×10^4	3.02×10^4	3.12×10^4	5.04×10^4	1.01×10^5	2.72×10^5
k_{-7} (i17 \rightarrow i2)	8.86×10^{12}	8.86×10^{12}	8.88×10^{12}	9.06×10^{12}	9.32×10^{12}	9.66×10^{12}
k_8 (i2 \rightarrow p2+H)	2.57×10^4	2.65×10^4	3.00×10^4	1.59×10^5	1.19×10^6	1.28×10^7
k_9 (i2 \rightarrow i12)	1.87	1.94	2.26	1.57×10^1	1.35×10^2	1.53×10^3
k_{-9} (i12 \rightarrow i2)	3.39×10^8	3.50×10^8	3.98×10^8	1.92×10^9	9.68×10^9	5.07×10^{10}
k_{10} (i17 \rightarrow i3)	2.26×10^{12}	2.26×10^{12}	2.29×10^{12}	2.65×10^{12}	3.22×10^{12}	4.10×10^{12}
k_{-10} (i3 \rightarrow i17)	2.50×10^7	2.52×10^7	2.62×10^7	4.57×10^7	1.00×10^8	2.93×10^8
k_{11} (c2 \rightarrow i3)	1.83×10^{11}	1.84×10^{11}	1.87×10^{11}	2.36×10^{11}	3.33×10^{11}	5.39×10^{11}
k_{-11} (i3 \rightarrow c2)	2.83×10^{10}	2.84×10^{10}	2.91×10^{10}	4.05×10^{10}	6.60×10^{10}	1.33×10^{11}
k_{12} (c2 \rightarrow i8)	7.90×10^{10}	7.92×10^{10}	7.98×10^{10}	8.92×10^{10}	1.05×10^{11}	1.33×10^{11}

TABLE I. (Continued.)

	0.0	0.03	0.15	2.0	5.0	10.0
k_{-12} (i8 \rightarrow c2)	2.51×10^{13}	2.52×10^{13}	2.52×10^{13}	2.65×10^{13}	2.85×10^{13}	3.15×10^{13}
k_{13} (c2 \rightarrow c3)	3.87×10^9	3.89×10^9	3.99×10^9	5.70×10^9	9.43×10^9	1.87×10^{10}
k_{-13} (c3 \rightarrow c2)	1.62×10^{10}	1.63×10^{10}	1.66×10^{10}	2.14×10^{10}	3.05×10^{10}	4.88×10^{10}
k_{14} (c2 \rightarrow i5)	2.36×10^8	2.37×10^8	2.42×10^8	3.38×10^8	5.40×10^8	1.03×10^9
k_{-14} (i5 \rightarrow c2)	9.21×10^{11}	9.23×10^{11}	9.33×10^{11}	1.08×10^{12}	1.31×10^{12}	1.70×10^{12}
k_{15} (c4 \rightarrow i8)	7.74×10^{11}	7.75×10^{11}	7.80×10^{11}	8.57×10^{11}	9.69×10^{11}	1.13×10^{12}
k_{-15} (i8 \rightarrow c4)	9.11×10^{10}	9.18×10^{10}	9.43×10^{10}	1.40×10^{11}	2.40×10^{11}	4.89×10^{11}
k_{16} (c4 \rightarrow c5)	5.14×10^{11}	5.16×10^{11}	5.26×10^{11}	6.80×10^{11}	9.40×10^{11}	1.38×10^{12}
k_{-16} (c5 \rightarrow c4)	4.54×10^3	4.60×10^3	4.83×10^3	9.84×10^3	2.61×10^4	9.49×10^4
k_{17} (c5 \rightarrow i10)	2.02×10^6	2.03×10^6	2.07×10^6	2.81×10^6	4.40×10^6	8.37×10^6
k_{-17} (i10 \rightarrow c5)	2.03×10^{12}	2.03×10^{12}	2.06×10^{12}	2.42×10^{12}	3.06×10^{12}	4.25×10^{12}
k_{18} (c5 \rightarrow i9)	5.03×10^5	5.06×10^5	5.19×10^5	7.46×10^5	1.27×10^6	2.68×10^6
k_{-18} (i9 \rightarrow c5)	9.35×10^{12}	9.35×10^{12}	9.37×10^{12}	9.59×10^{12}	9.92×10^{12}	1.04×10^{13}
k_{19} (c5 \rightarrow i5)	3.30×10^2	3.35×10^2	3.53×10^2	7.54×10^2	2.12×10^3	8.28×10^3
k_{-19} (i5 \rightarrow c5)	5.42×10^{10}	5.46×10^{10}	5.65×10^{10}	9.11×10^{10}	1.70×10^{11}	3.64×10^{11}
k_{20} (i10 \rightarrow i9)	1.79×10^{11}	1.80×10^{11}	1.83×10^{11}	2.31×10^{11}	3.24×10^{11}	5.15×10^{11}
k_{-20} (i9 \rightarrow i10)	3.46×10^{12}	3.46×10^{12}	3.47×10^{12}	3.60×10^{12}	3.80×10^{12}	4.07×10^{12}
k_{21} (i10 \rightarrow i9')	1.21×10^{11}	1.22×10^{11}	1.24×10^{11}	1.58×10^{11}	2.23×10^{11}	3.58×10^{11}
k_{-21} (i9' \rightarrow i10)	1.25×10^{12}	1.25×10^{12}	1.26×10^{12}	1.30×10^{12}	1.37×10^{12}	1.47×10^{12}
k_{22} (i5 \rightarrow i3)	6.61×10^{11}	6.64×10^{11}	6.74×10^{11}	8.32×10^{11}	1.11×10^{12}	1.75×10^{12}
k_{-22} (i3 \rightarrow i5)	2.61×10^7	2.64×10^7	2.73×10^7	4.47×10^7	9.04×10^7	2.60×10^8
k_{23} (c2 \rightarrow i3)	1.83×10^{11}	1.84×10^{11}	1.87×10^{11}	2.36×10^{11}	3.33×10^{11}	5.39×10^{11}
k_{-23} (i3 \rightarrow c2)	2.83×10^{10}	2.84×10^{10}	2.91×10^{10}	4.05×10^{10}	6.60×10^{10}	1.33×10^{11}
k_{24} (c1 \rightarrow i21)	3.17×10^7	3.21×10^7	3.33×10^7	5.89×10^7	1.30×10^8	3.79×10^8
k_{-24} (i21 \rightarrow c1)	2.07×10^{12}	2.08×10^{12}	2.11×10^{12}	2.62×10^{12}	3.47×10^{12}	4.93×10^{12}
k_{25} (c4 \rightarrow c6)	3.16×10^{11}	3.18×10^{11}	3.24×10^{11}	4.21×10^{11}	5.87×10^{11}	8.71×10^{11}
k_{-25} (c6 \rightarrow c4)	1.27×10^7	1.29×10^7	1.34×10^7	2.51×10^7	5.82×10^7	1.73×10^8

TABLE I. (Continued.)

	0.0	0.03	0.15	2.0	5.0	10.0
k_{26} (c5→c6)	1.92×10^8	1.93×10^8	1.94×10^8	2.13×10^8	2.45×10^8	3.02×10^8
k_{-26} (c6→c5)	1.15×10^{12}	1.15×10^{12}	1.15×10^{12}	1.16×10^{12}	1.18×10^{12}	1.21×10^{12}
k_{27} (c6→i2)	2.22×10^{12}	2.22×10^{12}	2.22×10^{12}	2.24×10^{12}	2.27×10^{12}	2.31×10^{12}
k_{-27} (i2→c6)	9.63×10^8	9.66×10^8	9.76×10^8	1.14×10^9	1.45×10^9	2.07×10^9
k_{28} (c6→i21)	4.45×10^5	4.54×10^5	4.94×10^5	1.55×10^6	6.38×10^6	3.47×10^7
k_{-28} (i21→c6)	3.00×10^{10}	3.05×10^{10}	3.25×10^{10}	7.64×10^{10}	2.09×10^{11}	6.43×10^{11}
k_{29} (i10→i21)	2.13×10^9	2.15×10^9	2.23×10^9	3.71×10^9	7.42×10^9	1.82×10^{10}
k_{-29} (i21→i10)	6.51×10^{11}	6.54×10^{11}	6.67×10^{11}	8.75×10^{11}	1.25×10^{12}	1.92×10^{12}

collision energy. In addition to the most efficient c5→c6 channel with the corresponding $k_{26}=1.92 \times 10^8 \text{ s}^{-1}$, which is to be described in the next section, consumption of c5 could also be achieved through reactions of c5→C+HCCCN, c5→c4, and c5→i5, though in a much slower pace with the corresponding rate constants, k_{c5} , k_{-16} , and k_{19} , being 9.29×10^3 , 4.54×10^3 , and $3.30 \times 10^2 \text{ s}^{-1}$, respectively, at 0.0 collision energy. It is obvious at low collision energy, c5 is around two times more likely to directly decompose to reactants than via another complex c4, in which the latter leads mostly to the same reactants and to a lesser extent to p2+H. As for the least competitive channel, the c5 ring closing to i5, out of whose five possible ring openings producing c2, i3, c5, i9, and i7, respectively, and the 1,2 H-migration to i12, the most probable path would take i5 to c2 and subsequently, p2+H.

H. Reaction paths of aziridine-1,2-diene-3-ylidene-ethene-1-yl (c6)

Five channels are characterized for c6: three possible ring openings to i2, c5, and c4, CNC ring closing to i21, and carbon decomposition to the reactants C+HCCCN. The possible H-dissociation products, aziridinylidene-3-ene-3-ylidene-1-ylidene (p11)+H, are located at 33.7 kcal/mol, which is clearly not feasible at ultralow temperature; at current level of theory, failed attempts in finding the intermediate for c6 H shift seem to suggest that the channel is not open.

The RRKM calculations indicate that c6 is very unstable with respect to both conversions to i2 and c5, as revealed by their large rate constants k_{27} and k_{-26} , being 2.22×10^{12} and $1.15 \times 10^{12} \text{ s}^{-1}$ at 0.0 collision energy, respectively. The next competitive channels of c6→C+HCCCN and c6→c4 appear insignificant with the k_{c6} and k_{-25} almost five orders of magnitude smaller. The ring formation back to c6 turns out to be the most energetically and kinetically favored path for c5 as described above. On the other hand, i2 would ultimately lead c6 to p2+H, as discussed in Sec. III C.

I. The most probable paths of C(³P)+HCCCN reaction

Figure 11 reveals the most probable paths inferred and thus the reaction mechanisms of c1–c6, respectively, at ultralow temperatures and in the environments where only single binary collision is permitted, such as cold molecular clouds and crossed-beam experiments. All the paths in Fig. 11 are of energy lower than the reactants, C(³P)+HCCCN, and obviously not all the paths with energy below the reactants in Figs. 5–10 are present. It would be logical that the most probable paths are the most kinetically competitive.

For c1, only the minimum energy path to i2 is kept; up to five channels of i2 have to be included in order to incorporate the reaction leading to the dissociation products, p2+H. Likewise, the determinations for c3 and c5 are straightforward, namely, of which the most probable paths comprise the species along the minimum energy paths that immediately bring c1 and c6, respectively. For c2 and c6, the second minimum energy path is also included, which makes both i2 and c1 immediate intermediates for the former, and i2 and c5 for the latter. c2, c3, c5, and c6 eventually yield the same products, p2+H.

Being singularly different, the final destination of c4 is mainly the carbon decomposition products, C+HCCCN, while p2+H are the second major products. Three immediate channels are taken in for c4: the most kinetically favored c4→C+HCCCN, the minimum energy path c4→i8, and its kinetic rival c4→c5, in which the latter two generate p2+H almost exclusively. At 0.0 collision energy, the corresponding rate constants k_{c4} , k_{15} , and k_{16} are in a ratio of 3.7:1.5:1. Overall for c4, the yields of C+HCCCN and p2+H are nearly 3:2.

Accordingly, in Fig. 12, the energetically and kinetically favored channels of c1–c6 revealed in Fig. 11 are assembled to give the most probable paths for the C(³P)+HCCCN reaction. It can be gathered that collision complexes, c1, c2, c3, c5, and c6, progressing through a common and the most stable intermediate i2, the most stable species due to dissociation, p2, emerges as the single most important product. On

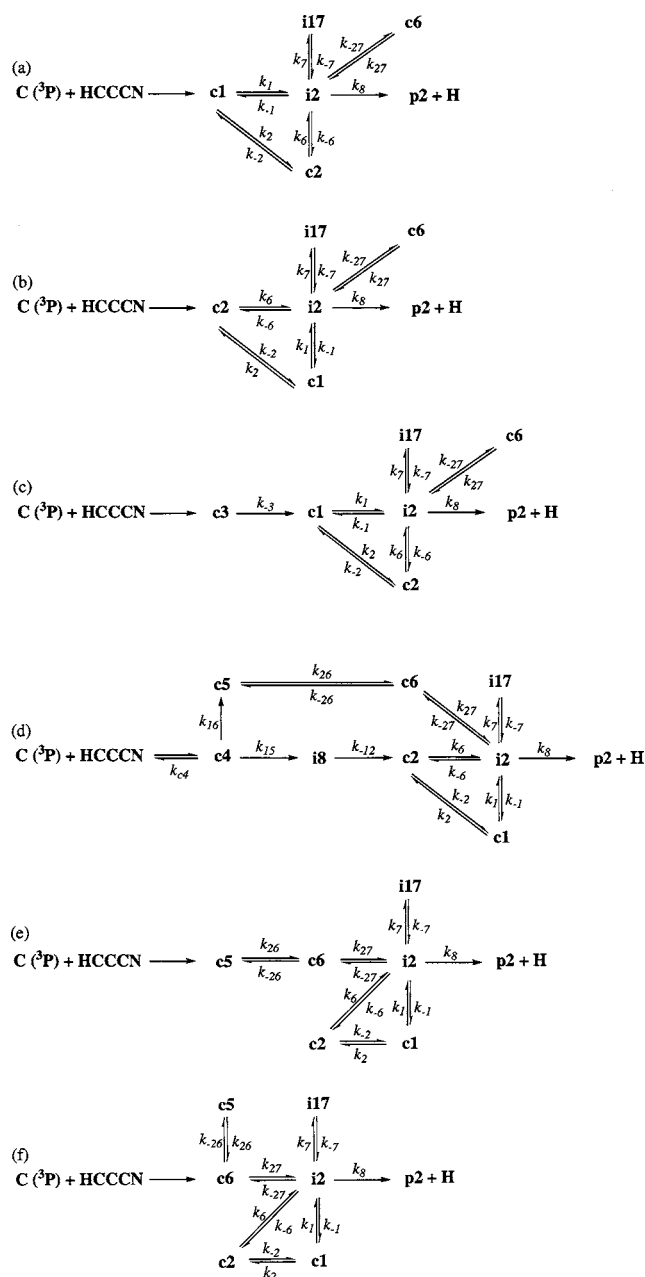


FIG. 11. The schematic diagrams [(a)–(f)] for the most probable paths of collision complexes c1–c6, respectively, in which the k 's are the corresponding rate constants.

the other hand, for the least stable collision complex c4, the kinetically advantageous $C+HCCCN$ is the major product despite being thermodynamically less stable than $p2+H$ which attributes 40% of the yield.

IV. CONCLUSION

The reaction of the ground-state carbon atom ($C(^3P)$ with a prototype cyanoacetylene ($HCCCN(X^1\Sigma^+)$) molecule has been investigated by employing *ab initio* electronic structure calculations and RRKM theory. For the relevancy of the titled reaction occurring at ultralow temperature as in interstellar medium, the reaction paths of barrierless entrance channels on the adiabatic triplet ground-state potential-energy surface of C_4HN are sought out and characterized.

The optimized geometries and harmonic frequencies for the collision complexes, intermediates, transition states, and dissociation products are obtained with the unrestricted B3LYP/6-311G(*d,p*) calculations; the corresponding CCSD(T)/cc-pVTZ energies with the unrestricted B3LYP/6-311G(*d,p*) zero-point energy corrections have been computed. Six collision complexes, c1–c6, are located; the isomerization and dissociation channels of each complex are identified and scrutinized. Six one-dimensional potential-energy curves which closely follow the reaction coordinates for c1–c6 decomposition back to $C+HCCCN$, respectively, have also been mapped out with the IRC calculations at B3LYP/6-311G(*d,p*) level. Based on the *ab initio* potential-energy surface, specifically the B3LYP/6-311G(*d,p*) harmonic frequencies and the CCSD(T)/cc-pVTZ energies, the rate constants for important elementary steps have been predicted according to the RRKM and variational RRKM theories at collision energies of 0.0, 0.03, 0.15, 2, 5, and 10 kcal/mol. The most probable paths for the six collision complexes, respectively, are determined with utilization of the predicted rate constants; collectively, they constitute the most probable paths for the $C(^3P)+HCCCN(X^1\Sigma^+)$ reaction.

Present study indicates that although there are two possible hydrogen atom-dissociation products, three-membered p1 and linear p2, with energies below the reactants, the energetically more stable p2 appears to be the sole product for H decomposition. Via the linear and most stable intermediate, i2, five collision complexes, c1, c2, c3, c5, and c6, all end up at one single final product, $p2+H$, with a near 100% yield. Though not of as big a share, p2 is also a significant final product of the collision complex, c4, with 40% yield. Our work suggests that the most likely channel for c4 is in fact the reversed reaction to $C+HCCCN$, which accounts for 60% of the final yields. The consequence would not be obvious with the knowledge of potential-energy surface alone, which exemplifies the merit of a combination with kinetics study in predicting the outcome of a seemingly simple reaction. The branching ratios of the most probable products, $p2+H$ and $C+HCCCN$, for the titled reaction would not be fully realized without the bimolecular rate constants for the formation of collision complexes, c1–c6, respectively, the address of which is of fundamental importance and currently under way in our laboratory, and has potentially various applications in barrierless multichannel reactions in general. Nevertheless, it is of great interest to compare the results with the experiment, especially, the crossed-beam investigation, to assess not only the H-dissociation products but also the surprising prediction of the $C+HCCCN$ as final products.

For the titled reaction, this work establishes a detailed picture of the products and short-lived intermediates, identifies the most probable paths below the energy of the separated reactants, and predicts the most likely products. The investigation suggests that this class of reaction is very likely an important route to the destruction of the well-known interstellar molecules, cyanopolynes, and to the synthesis of linear carbon-chained nitriles at the temperature as low as

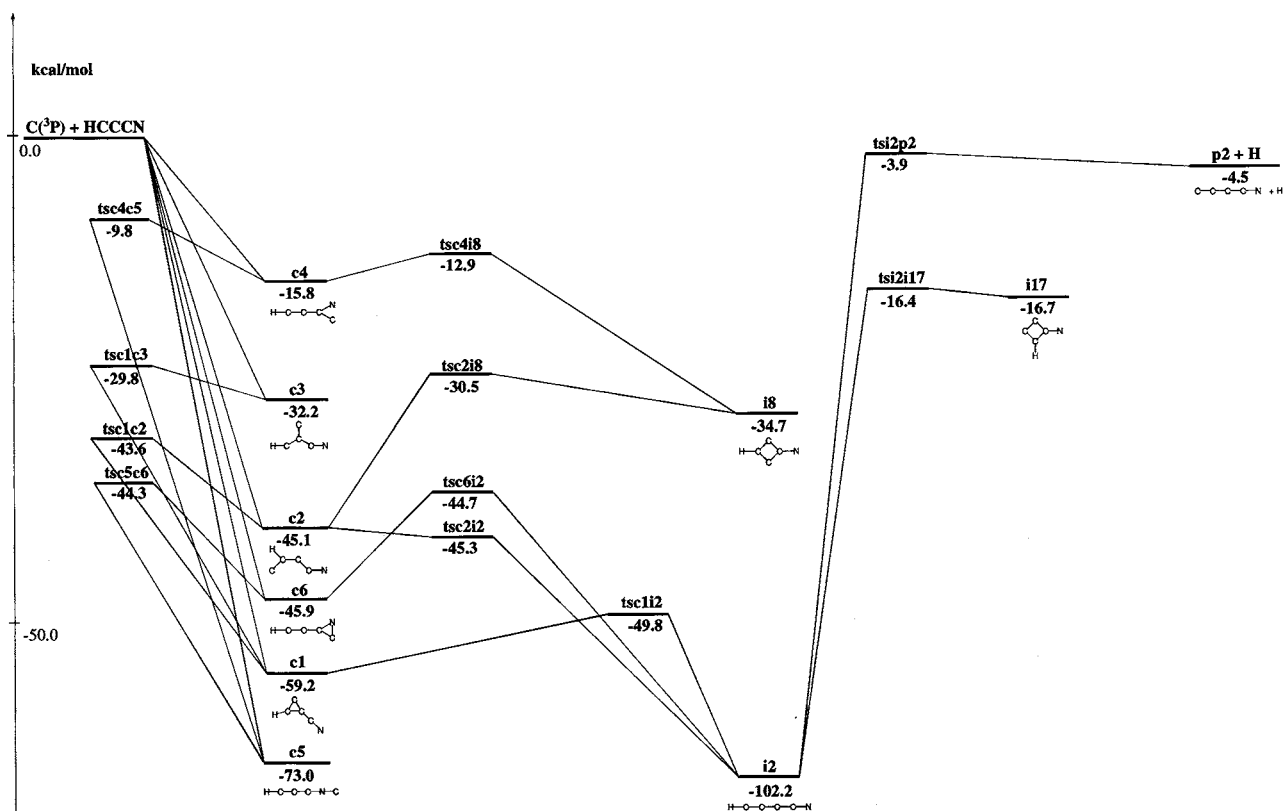


FIG. 12. The most probable paths of the $C(^3P)+HCCCN(X^1\Sigma^+)$ reaction as indicated in Fig. 11, in which the energies in kcal/mol relative to the reactants, $C(^3P)+HCCCN(X^1\Sigma^+)$, are computed with CCSD(T)/cc-pVTZ level of theory with B3LYP/6-311G(*d,p*) zero-point energy corrections at the B3LYP/6-311G(*d,p*) optimized geometries, as shown in Figs. 1–4.

10 K, and that the results of the current investigation should be incorporated in future chemical models of interstellar clouds.

ACKNOWLEDGMENTS

This work was supported by the National Science Council of Taiwan (Grant NSC 93-2113-M-259-010). Computer resources at the National Center for High-Performance Computer of Taiwan were utilized in parts of the calculations. We thank the referee for the stimulating comments.

- ¹N. Haider and D. Husain, *Z. Phys. Chem.* **176**, 133 (1992).
- ²N. Haider and D. Husain, *J. Chem. Soc., Faraday Trans.* **89**, 7 (1993).
- ³N. Haider and D. Husain, *J. Photochem. Photobiol., A* **70**, 119 (1993).
- ⁴N. Haider and D. Husain, *Combust. Flame* **93**, 327 (1993).
- ⁵D. C. Clary, N. Haider, D. Husain, and M. Kabir, *Astrophys. J.* **422**, 416 (1994).
- ⁶D. Husain and A. X. Ioannou, *J. Chem. Soc., Faraday Trans.* **93**, 3620 (1997).
- ⁷D. A. Lichtin and M. C. Lin, *Chem. Phys.* **96**, 473 (1985).
- ⁸D. L. Yang, T. Yu, N. S. Wang, and M. C. Lin, *Chem. Phys.* **160**, 317 (1992).
- ⁹K. Seki, M. Yagi, M. He, J. B. Halpern, and H. Okabe, *Chem. Phys. Lett.* **258**, 657 (1996).
- ¹⁰I. R. Sims, J.-L. Queffelec, D. Travers, B. R. Rowe, L. B. Herbert, J. Karthaus, and I. W. M. Smith, *Chem. Phys. Lett.* **211**, 461 (1993).
- ¹¹D. Chastaing, P. L. James, I. R. Sims, and I. W. M. Smith, *Phys. Chem. Chem. Phys.* **1**, 2247 (1999).
- ¹²I. W. M. Smith and B. Rowe, *Acc. Chem. Res.* **33**, 261 (2000).
- ¹³E. Herbst, *Annu. Rev. Phys. Chem.* **46**, 27 (1995).
- ¹⁴R. P. A. Bettens, H.-H. Lee, and E. Herbst, *Astrophys. J.* **443**, 664 (1995).
- ¹⁵E. Herbst, H.-H. Lee, D. A. Howe, and T. J. Millar, *Mon. Not. R. Astron. Soc.* **268**, 335 (1994).
- ¹⁶E. Herbst, *Chem. Soc. Rev.* **30**, 168 (2001).
- ¹⁷R. I. Kaiser, Y. T. Lee, and A. G. Suits, *J. Chem. Phys.* **103**, 10395 (1995).
- ¹⁸R. I. Kaiser, Y. T. Lee, and A. G. Suits, *J. Chem. Phys.* **105**, 8705 (1996).
- ¹⁹R. I. Kaiser, C. Ochsenfeld, M. Head-Gordon, Y. T. Lee, and A. G. Suits, *Science* **274**, 1508 (1996).
- ²⁰R. I. Kaiser, D. Stranges, Y. T. Lee, and A. G. Suits, *J. Chem. Phys.* **105**, 8721 (1996).
- ²¹R. I. Kaiser, C. Ochsenfeld, M. Head-Gordon, Y. T. Lee, and A. G. Suits, *J. Chem. Phys.* **106**, 1729 (1997).
- ²²R. I. Kaiser, D. Stranges, H. M. Bevsek, Y. T. Lee, and A. G. Suits, *J. Chem. Phys.* **106**, 4945 (1997).
- ²³R. I. Kaiser, D. Stranges, Y. T. Lee, and A. G. Suits, *Astrophys. J.* **477**, 982 (1997).
- ²⁴R. I. Kaiser, A. M. Mebel, A. H. H. Chang, S. H. Lin, and Y. T. Lee, *J. Chem. Phys.* **110**, 10330 (1999).
- ²⁵R. I. Kaiser, I. Hahndorf, L. C. L. Huang, Y. T. Lee, H. F. Bettinger, P. V. Schleyer, H. F. Schaefer, and P. R. Schreiner, *J. Chem. Phys.* **110**, 6091 (1999).
- ²⁶I. Hahndorf, H. Y. Lee, A. M. Mebel, S. H. Lin, Y. T. Lee, and R. I. Kaiser, *J. Chem. Phys.* **113**, 9622 (2000).
- ²⁷B. Balucani, H. Y. Lee, A. M. Mebel, Y. T. Lee, and R. I. Kaiser, *J. Chem. Phys.* **115**, 5107 (2001).
- ²⁸R. I. Kaiser, A. M. Mebel, and Y. T. Lee, *J. Chem. Phys.* **114**, 231 (2001).
- ²⁹R. I. Kaiser, T. L. Nguyen, A. M. Mebel, and Y. T. Lee, *J. Chem. Phys.* **116**, 1318 (2002).
- ³⁰I. Hahndorf, Y. T. Lee, R. I. Kaiser, L. Vereecken, J. Peeters, H. F. Bettinger, W. D. Allen, and H. F. Schaefer III, *J. Chem. Phys.* **116**, 3248 (2002).
- ³¹R. I. Kaiser and N. Balucani, *Acc. Chem. Res.* **34**, 699 (2001).
- ³²E. Herbst and C. M. Leung, *Astron. Astrophys.* **233**, 177 (1990).
- ³³K. Fukuzawa and Y. Osamura, *Astrophys. J.* **489**, 113 (1997).
- ³⁴K. Fukuzawa, Y. Osamura, and H. F. Schaefer, *Astrophys. J.* **505**, 278 (1998).
- ³⁵L. C. L. Huang, N. Balucani, Y. T. Lee, R. I. Kaiser, and Y. Osamura, *J. Chem. Phys.* **111**, 2857 (1999).

- ³⁶N. Balucani, O. Asvany, A. H. H. Chang, S. H. Lin, Y. T. Lee, R. I. Kaiser, H. F. Bettinger, P. v. R. Schleyer, and H. F. Schaefer, *J. Chem. Phys.* **111**, 7472 (1999).
- ³⁷N. Balucani, O. Asvany, A. H. H. Chang, S. H. Lin, Y. T. Lee, R. I. Kaiser, H. F. Bettinger, P. v. R. Schleyer, and H. F. Schaefer, *J. Chem. Phys.* **111**, 7457 (1999).
- ³⁸N. Balucani, O. Asvany, A. H. H. Chang, S. H. Lin, Y. T. Lee, R. I. Kaiser, and Y. Osamura, *J. Chem. Phys.* **113**, 8643 (2000).
- ³⁹L. C. L. Huang, A. H. H. Chang, O. Asvany, N. Balucani, S. H. Lin, Y. T. Lee, R. I. Kaiser, and Y. Osamura, *J. Chem. Phys.* **113**, 8656 (2000).
- ⁴⁰N. Balucani, O. Asvany, L. C. L. Huang, Y. T. Lee, R. I. Kaiser, Y. Osamura, and H. F. Bettinger, *Astrophys. J.* **545**, 892 (2000).
- ⁴¹N. Balucani, O. Asvany, Y. T. Lee, R. I. Kaiser, and Y. Osamura, *J. Phys. Chem. A* **106**, 4301 (2002).
- ⁴²H. F. Su, R. J. Kaiser, and A. H. H. Chang, *J. Chem. Phys.* **122**, 074320 (2005).
- ⁴³B. E. Turner, *Astrophys. J.* **163**, L35 (1971).
- ⁴⁴N. W. Broten *et al.*, *Astrophys. J.* **276**, L25 (1984).
- ⁴⁵M. B. Bell, P. A. Feldman, M. J. Travers, M. C. McMarthy, C. A. Gottlieb, and P. Thaddeus, *Astrophys. J.* **483**, L61 (1997).
- ⁴⁶M. B. Bell, J. K. G. Watson, P. A. Feldman, and M. J. Travers, *Astrophys. J.* **508**, 286 (1998).
- ⁴⁷A. D. Becke, *J. Chem. Phys.* **98**, 5648 (1993); **96**, 2155 (1992); **97**, 9173 (1992); C. Lee, W. Yang, and R. G. Parr, *Phys. Rev. B* **37**, 785 (1988).
- ⁴⁸G. D. Purvis and R. J. Bartlett, *J. Chem. Phys.* **76**, 1910 (1982); C. Hampel, K. A. Peterson, and H.-J. Werner, *Chem. Phys. Lett.* **190**, 1 (1992); P. J. Knowles, C. Hampel, and H.-J. Werner, *J. Chem. Phys.* **99**, 5219 (1994); M. J. O. Deegan and P. J. Knowles, *Chem. Phys. Lett.* **227**, 321 (1994).
- ⁴⁹M. J. Frisch *et al.*, GAUSSIAN 98, Revision A.5, Gaussian, Inc., Pittsburgh, PA, 1998.
- ⁵⁰H. Eyring, S. H. Lin, and S. M. Lin, *Basic Chemical Kinetics* (Wiley, New York, 1980).
- ⁵¹A. H. H. Chang, A. M. Mebel, X.-M. Yang, S. H. Lin, and Y. T. Lee, *J. Chem. Phys.* **109**, 2748 (1998).
- ⁵²W. L. Hase, *Acc. Chem. Res.* **16**, 258 (1983).
- ⁵³R. A. Marcus, *Chem. Phys. Lett.* **144**, 208 (1988).
- ⁵⁴A. H. H. Chang, D. W. Hwang, X. M. Yang, A. M. Mebel, S. H. Lin, and Y. T. Lee, *J. Chem. Phys.* **110**, 10810 (1999).
- ⁵⁵See EPAPS Document No. E-JCPA6-123-019548 for the illustrations of Fig. s1 and Table sI. This document can be reached via a direct link in the online article's HTML reference section or via the EPAPS homepage (<http://www.aip.org/pubservs/epaps.html>).
- ⁵⁶C. Ochsenfeld, R. I. Kaiser, Y. T. Lee, A. G. Suite, and M. Head-Gordon, *J. Chem. Phys.* **106**, 4141 (1997).